Hygroscopic Optical Growth of Atmospherically Relevant Mixed Particles

by

Carly B. Robinson

B.A. Michigan Technological University, 2007

M.S. University of Colorado, 2010

A thesis submitted to the

faculty of the Graduate School of the

University of Colorado in partial fulfillment

of the requirements for the degree of

Doctor of Philosophy

Department of Chemistry & Biochemistry

2013

The thesis entitled:

Hygroscopic Optical Growth of Atmospherically Relevant Mixed Particles

written by Carly B. Robinson

has been approved for the Department of Chemistry and Biochemistry.

_____

Dr. Margaret A. Tolbert

_____

Dr. Veronica Bierbaum

Date _____

The final copy of this thesis has been examined by the signatories, and we find that both the content and the form meet acceptable presentation standards of the scholarly work in the above mentioned discipline.

Carly B. Robinson (Ph.D. Chemistry and Biochemistry)

Hygroscopic Optical Growth of Atmospherically Relevant Mixed Particles

Thesis directed by Professor Margaret A. Tolbert

The direct interaction of ambient atmospheric particles with solar radiation affects Earth's climate and local visibility. Light extinction by particles in the atmosphere is strongly dependent on particle size, chemical composition, hygroscopic growth properties and particle mixing state. Changes in relative humidity can influence particle extinction because hygroscopic growth causes the particles to increase in size. Laboratory quantification of the optical growth of various particle compositions is needed for inclusion in radiative transfer models. While the optical growth of pure particles is well understood, less is known about mixed particles. Atmospheric aerosols are typically 50-80% organic, but also contain sulfates. This thesis describes laboratory investigations into the role of organics on the optical hygroscopic growth of ammonium sulfate (AS).

The influence of an organic 1,2,6-hexanetriol coating on an ammonium sulfate particle was first studied. The particle optical growth factor, $f\mathrm{RH}_{\mathrm{ext}}$, was measured using cavity ring-down aerosol extinction spectroscopy at 532 nm. The particles were composed of pure ammonium sulfate, pure 1,2,6-hexanetriol, and mixed particles containing a wet or dry ammonium sulfate core and 1,2,6-hexanetriol coating. Dry, coated particles were generated by atomization followed by drying. Wet, coated particles were formed via liquid-liquid phase separation (LLPS). LLPS was achieved by deliquescing the mixed particles, and then the particles were dried to a relative humidity (RH) between the phase separation RH and the efflorescence RH. For the LLPS particles, the $f\mathrm{RH}_{\mathrm{ext}}$ at each RH was found to be between the

fRH_{ext} of ammonium sulfate and 1,2,6-hexanetriol. In contrast, for the mixed dry, coated particles, the fRH_{ext} was the same as 1,2,6-hexanetriol particles. This work shows that at room temperature, the water uptake properties of AS coated with 1,2,6-hexanetriol are largely dictated by the phase of the AS. Thus, the total water uptake depends on the RH history of the particle and the resulting phase of AS.

The influence of adding semi-solid, glassy particles to AS particles on the particle optical growth was then studied. Particles were composed of ammonium sulfate (AS), 1,2,6-hexanetriol, sucrose, raffinose, and mixed particles containing AS and either sucrose or raffinose. Both sucrose and raffinose were used because they can be semi-solid or glassy at room temperature. For the pure 1,2,6-hexanetriol, sucrose, and raffinose, the particles optical growth begins to occur around an RH between 34 and 40%. The liquid 1,2,6-hexanetriol exhibits similar water uptake behavior as the glassy sucrose and raffinose. Therefore, pure glassy aerosols may be treated similar to liquids is climate change models. For the mixed AS and sucrose or raffinose particles, the component weight % significantly affects the RH where water uptake is observed. When particles contain more AS than organic, it acts similar to a pure AS particle. The AS in the mixture is crystalline, and the particle doesn't take up much water until it deliquesces. When the particle contains more organic, it acts like a liquid particle and has slow continuous water uptake. This significantly simplifies the addition of mixed glassy aerosols in climate change models.

For Dad, Mom, Kale, Laney,

my grandparents, aunts, uncles,

cousins and Nick.

Thank you for all your love

and support!

Acknowledgements

I am grateful to so many people who have helped me along this journey toward my Ph.D. First and foremost, I want to thank my family. My parents have instilled such a strong work ethic, making me believe I can accomplish anything I set my mind to. Without their support and push, I may not have achieved my goal of becoming a scientist. Kale and Laney, I love you both so much and am so proud of you. I also want to thank my Grandma Bobby, who has always been a model of female strength in my family. Without her support and help finding our way through the private student loan process, I would not have made it to Michigan Tech. I love you all so much and couldn't have made it this far without your love and support.

I also want to thank all of the professors and teachers I've had throughout my education. I was fortunate enough to attend the Macomb Academy of Arts and Science High School. I took accelerated math, science, and programming classes, which helped develop my interest in physics. My senior research project was delving into string theory; not an easy task for a 17 year old. But, after reading Brian Green's *The Elegant Universe*, I decided to study physics at Michigan Technological University.

I met Dr. Will Cantrell when I first arrived at Tech. He was an incredible mentor and teacher. He even convinced me to stay in physics at Tech during my sophomore year when I considered transferring to archeology. Without Dr. Cantrell, I would have never had the opportunity to work with Dr. Laura Iraci at NASA Ames and may have never learned about the extraordinary research being done at the University of Colorado. Laura introduced me to Maggie and the incredible research by the Tolbert group.

I am so thankful for my advisor, Dr. Maggie Tolbert. She has been an incredible teacher and mentor, and has helped me get through a very difficult situation at CU. Without her support and guidance, I may have never finished my Ph.D. It has been great to be a member of the Tolbert group. All of our group members are incredibly helpful and supportive. I especially want to thank Gregg Schill for all of the valuable discussions as I was trying to finish my last two papers. I also thank NASA for supporting this work and for providing my NESSF Fellowship.

Last, but certainly not least, I want to thank my amazing boyfriend, Nick Shockey. This year was stressful and hectic, but through it all, he has been my rock. He has constantly reminded me that I am strong enough and smart enough to achieve my goals. I am so excited to start our journey together in DC.

Contents

Chapter IV: Summary, Conclusions, and Future Directions

List of Tables

List of Figures

Chapter I: Introduction

Chapter II: Impact of Organic Coating on Optical Growth of Ammonium Sulfate Particles

Chapter III: Optical Growth of Glassy Organics Sulfate Particles

Chapter I

Introduction

Incoming sunlight into our atmosphere provides ultraviolet, visible, and infrared radiation to the Earth's atmosphere and surface. Understanding how this incoming solar radiation interacts with the atmosphere's complex composition is crucial to understanding how Earth's climate is changing. Light extinction by particles in the atmosphere is strongly dependent on particle size, chemical composition, hygroscopic growth properties, and particle mixing state. Changes in relative humidity affect particle extinction because of particle size changes due to hygroscopic growth.

Experiments presented in this thesis are designed to address outstanding questions about how incoming solar radiation interacts with atmospheric aerosol particles. This work is laboratory-based, but spurred by the need to better understand the processes in Earth's atmosphere radiative balance. Specifically, we use a cavity ring-down aerosol extinction spectroscopy (CRD-AES) to better understand the role of particle optical growth due to water uptake for mixed ammonium sulfate and organic particles (*Abbatt et al*., 2006).

1.1 Aerosol Climate Impact

To understand Earth's climate, we need to understand the balance of incoming solar radiation and outgoing terrestrial radiation. Earth's radiative balance is complex, as shown in

Figure 1.1. Incoming solar radiation can interact with atmospheric particles and be reflected back to space, or be reflected or absorbed by Earth's surface. Terrestrial radiation can also interact with atmospheric particles and be reflected back to the surface, or emitted into space. Atmospheric aerosols play a significant role in Earth's radiative balance. Aerosols are liquids or solids suspended in a gas, which can interact with incoming solar radiation by scattering and/or absorbing light. This interaction is known as the aerosol *direct effect*. In general, the sum of particle scattering and absorption cools the Earth's surface, shown in Figure 1.2. The magnitude of the direct effect on radiative forcing was estimated by the Intergovernmental Panel on Climate Change (IPCC) in 2007 to be -0.5 Wm^{-2} ± 0.40 Wm^{-2} (*Forster*, 2007). Although the IPCC estimated the direct effect, there are large uncertainties within this estimation. In order to reduce these uncertainties, better understanding of the chemical, physical, and optical properties of the particles is needed.

The *indirect effect* of particles on climate describes the aerosol particles' ability to influence the radiative properties of clouds. Aerosol particles can take up water and if these particles take up enough water, they become cloud droplets. Aerosols that form clouds are termed cloud condensation nuclei (CCN). With changing chemical composition, particle composition, and particle size, the cloud water content changes. As the water content changes, so does the cloud reflectivity and lifetime. The IPCC estimates that the magnitude of the aerosol particle indirect effect on radiative forcing is ~ -0.7 Wm^{-2} (*Forster*, 2007).

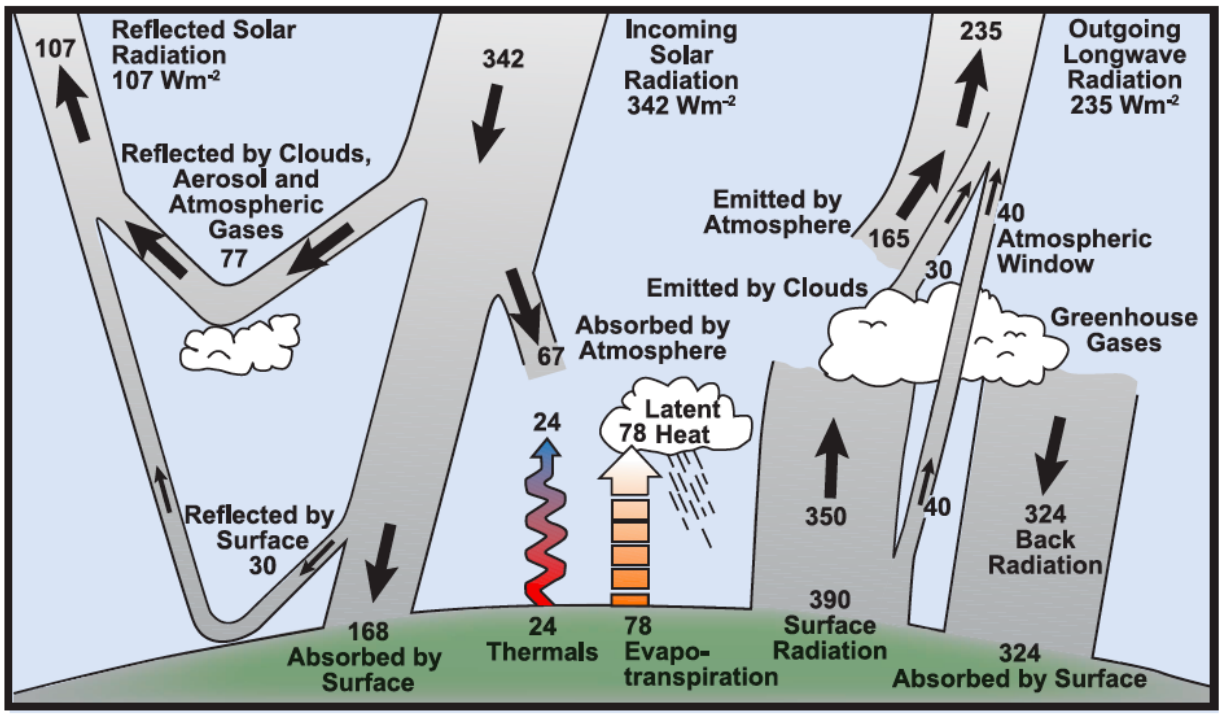

Figure 1.1 Estimate of Earth's annual and global mean energy balance. Figure from Forster et al. (2007).

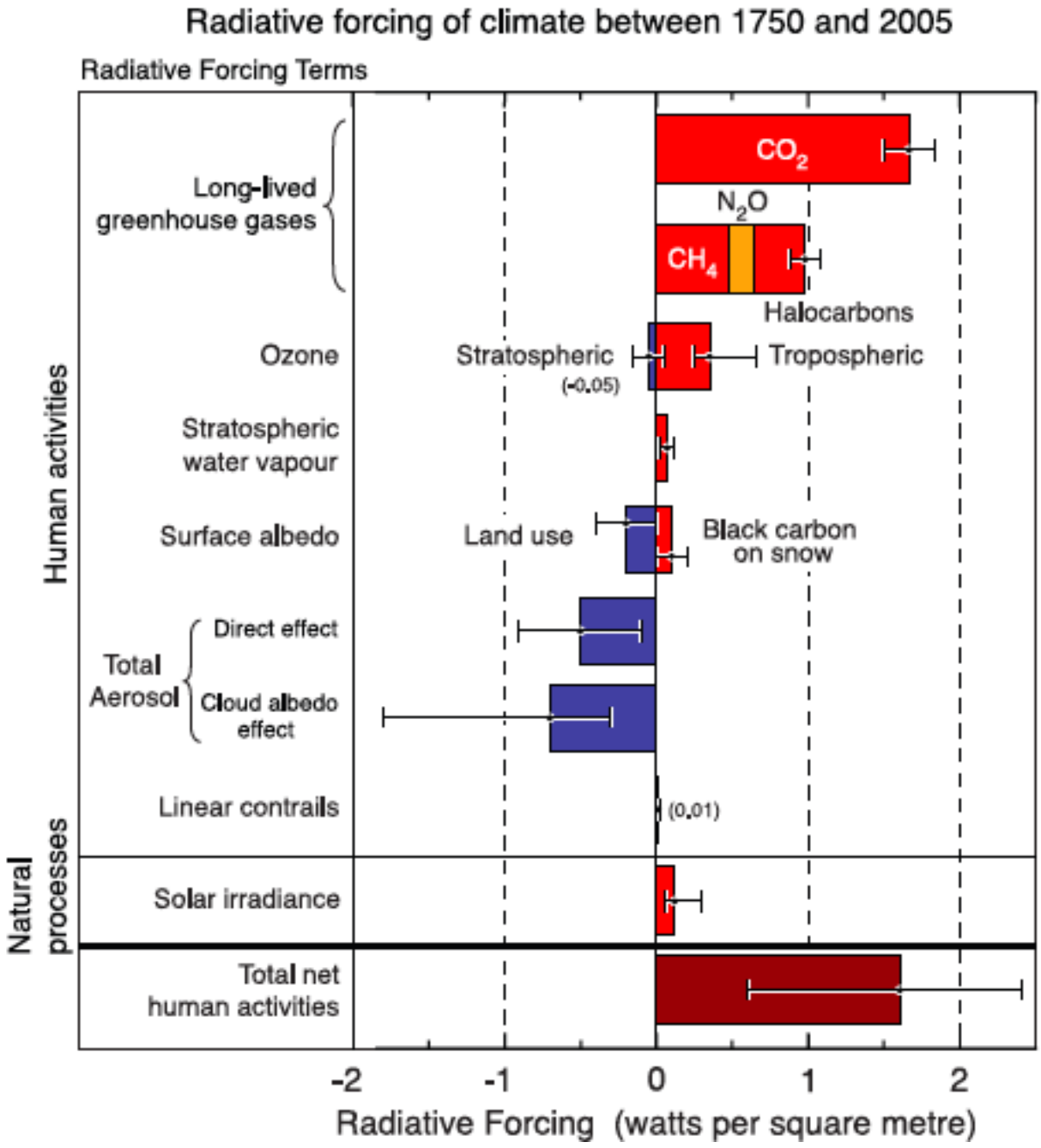

Figure 1.2 Summary of the Earth's radiative forcing from the IPCC 2007. Figure from Forster et al. (2007).

Relative humidity (RH) plays an important role in both the direct and indirect aerosol effects. As aerosol particles are transported in the atmosphere, there are changes in temperature and RH within the air parcel. With these changes, particles take up and release water. This will affect particles' direct interaction with incoming solar radiation, because their size and composition will be changing. These changes will affect the particles' optical properties, refractive index and optical growth factor. Indirectly, as these particles take up more and more water, and become cloud particles, they change the radiative balance even more.

Overall, the Earth is experiencing warming, but the cooling due to the radiative forcing of aerosol particles is off-setting this. There has been extensive research performed on both the direct and indirect aerosol effects, but there is still a lack of understanding because the atmosphere is so complex. The total overall error in the climate forcing is largely due to the errors in the total aerosol effect.

1.2 Chemical Composition of the Atmosphere

Atmospheric aerosols have a very complex chemical composition, shown in Figure 1.3 (*Zhang et al*., 2007). Measurements from around the world show that aerosols are made up of multiple components including both organics and inorganics. The inorganic fraction is better characterized and predicted than the organic fraction. Inorganics commonly found in aerosol particles include sulfates, nitrates, and ammonium. Ammonium sulfate (AS) is considered one of the most important inorganic salts found in mixed particles (*Finlayson-Pitts*, 2000; *Seinfeld*, 2006). Atmospheric sulfates are emitted into the atmosphere both naturally from oceans and volcanic activity, as well as through anthropogenic sources.

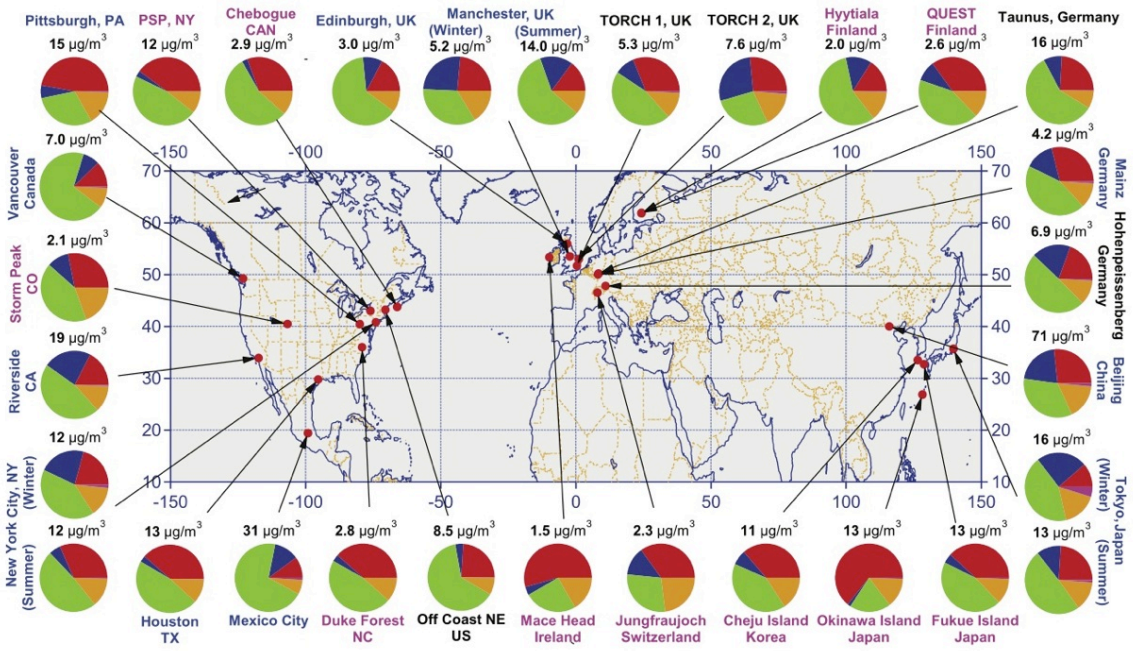

Figure 1.3 Field site locations of experiments use the Aerodyne Aerosol Mass Spectrometer and the aerosol chemical composition breakdown at each site with green for organics, red for sulfates, blue for nitrates, purple for chlorides, and gold for ammonium. Figure from Zhang et al. (2007).

The organic fraction of atmospheric aerosols is currently the subject of many research studies. Understanding the organic fraction's effect on climate is key to reducing the uncertainty in total aerosol radiative forcing. Organics make up 50-80% of the total aerosol composition (*Zhang et al.*, 2007). Organic aerosols can also be emitted into the atmosphere by natural and anthropogenic sources. There are thousands of organic species that have yet to be identified, but laboratory experiments probing different families of compounds are needed to achieve a better understanding of how they behave in the atmosphere.

Previous studies have also shown that both inorganic and organic components can be found in the same particle. Figure 1.4 shows mass spectra from a single particle, which contains both organic material and sulfates. While understanding how individual compounds interact in the atmosphere is important, to have a better understanding of the overall aerosol effect studies need to be performed using mixed organic and inorganic particles.

1.3 Particle Morphology and Liquid-Liquid Phase Separation (LLPS)

In addition to overall composition, particle morphology is also important to understanding atmospheric aerosols. Many climate models assume that particles of mixed composition are homogeneously mixed. That is, compounds have been considered to be evenly distributed within a particle. However, recent studies have shown that particles in the atmosphere often have coatings and are not purely homogeneously mixed. Not only do some atmospheric particles have coatings, but as the RH in the atmosphere changes, they can undergo liquid-liquid phase separation (LLPS). Agglomeration of coated particles may lead to even more complex heterogeneous mixtures.

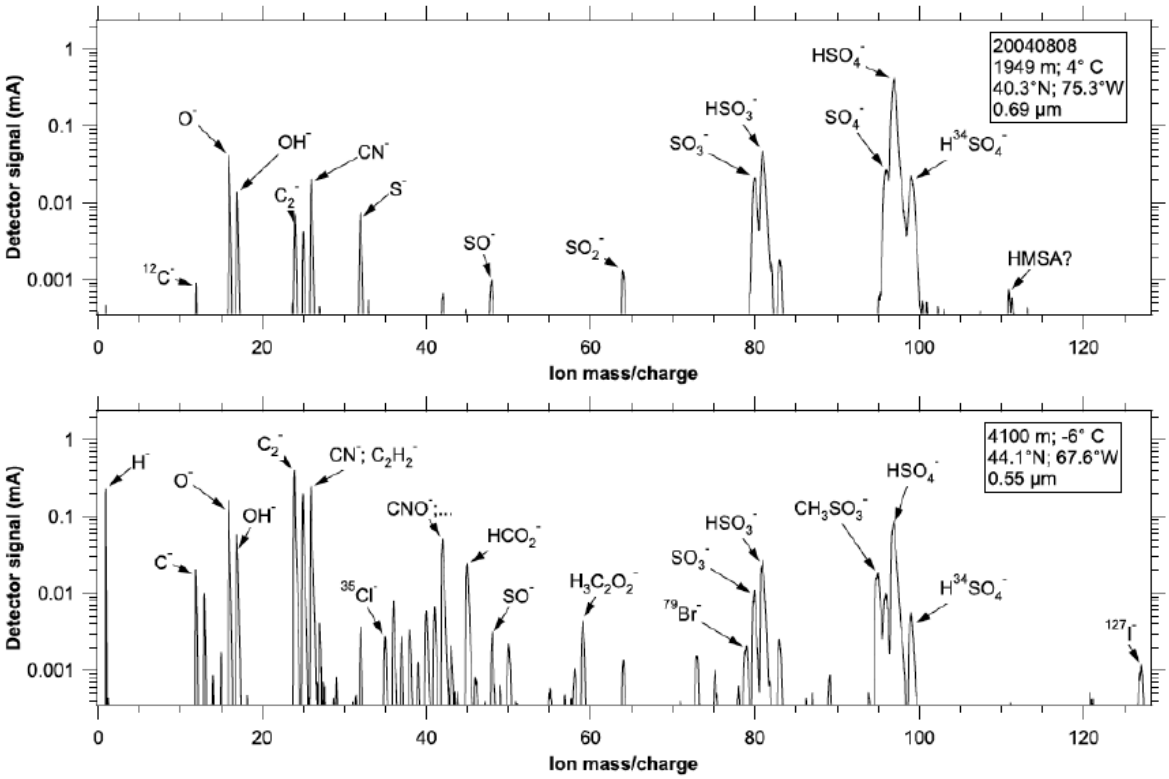

Figure 1.4 Single particle mass spectra from the PALMS instrument in positive and negative mode showing both sulfate and organic material in a single particle. The date, height, temperature, location, and particle size at which the particle was collected are also shown. Figure from Murphy et al. (2006).

Figure 1.5 shows the water uptake and loss behavior of a crystalline particle. As the RH is increased, crystalline particles are in a stable state until the RH reaches a characteristic level where the particle absorbs gas phase water until a saturated solution droplet is formed. This RH is termed the deliquescence relative humidity, DRH. As the RH is further increased, the particle continues to take up water. As the RH is decreased, the particle and gas phase water may be in equilibrium. Once the RH has passed below the DRH, the particles don't recrystallize immediately, because an initial nucleation step is needed to reform a crystalline solid. The particle remains in a metastable liquid state and is supersaturated until nucleation occurs and the particle recrystallizes. This RH is termed the efflorescence relative humidity, ERH.

For some particle mixtures, after deliquescence has occurred and the RH is decreased, a liquid-liquid phase separated state occurs. This observation has been made in previous studies and is shown in Figure 1.6 (*Bertram et al*., 2011). Initially, the particle is dry, at 0% RH and has a crystalline ammonium sulfate core and a liquid organic coating. As the RH is increased, the particle deliquesces. When the RH is decreased, LLPS occurs where a liquid organic coating surrounds an aqueous ammonium sulfate core. The RH at which LLPS occurs is defined as the separation relative humidity, SRH. As the RH continues to decrease, eventually the particle will effloresce. Bertram et al. showed that in multiple inorganic and organic mixtures, LLPS was observed in particles with O:C < 0.7. In contrast, particles with O:C > 0.7 did not undergo LLPS (*Bertram et al*., 2011).

A previous study has shown that LLPS is also possible in the atmosphere (*You et al*., 2012). Atmospheric particles were collected on filters, taken back to the lab, and extracted for

further analysis. Using optical and fluorescence microscopy, the particles were analyzed as the RH was cycled. Images show LLPS occurring of multiple particles composed of AS and organic

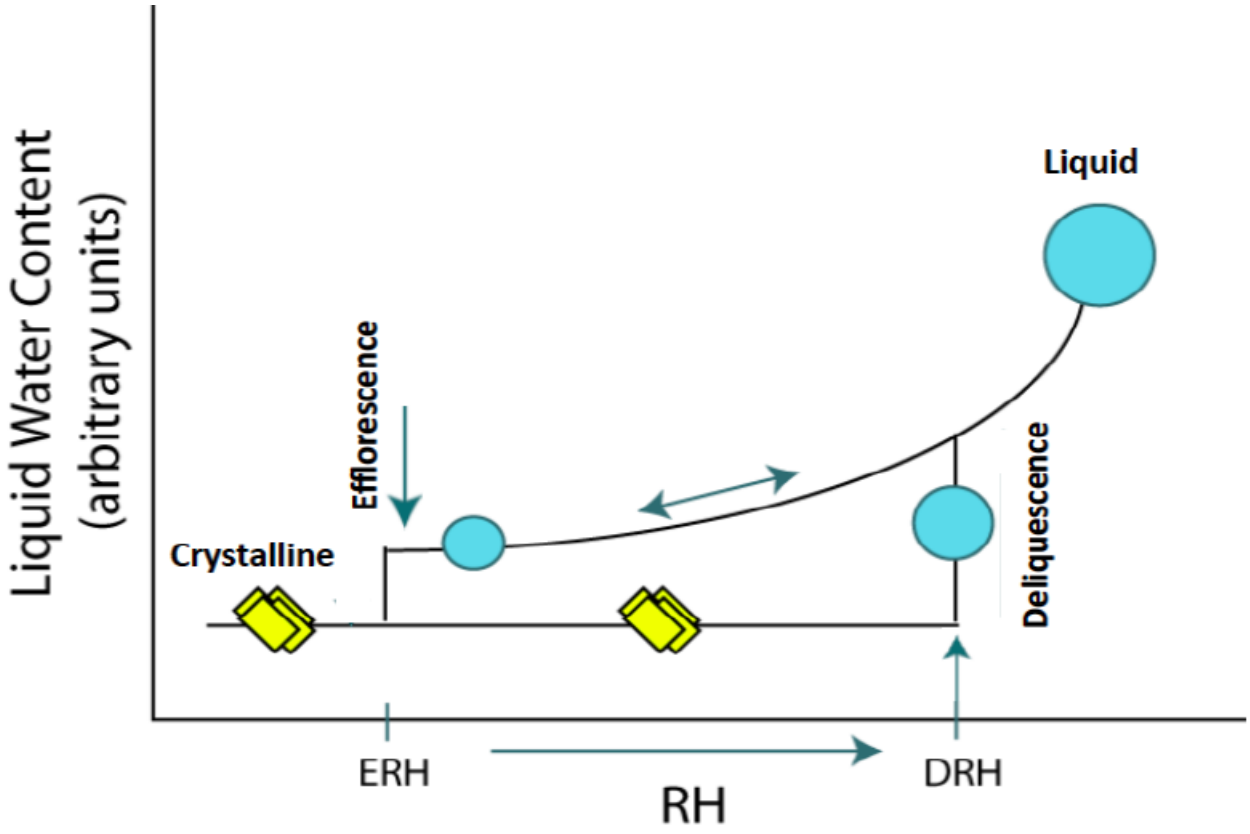

Figure 1.5 Particle liquid water content as a function of RH. The RH where the crystalline particle begins to take up water is the deliquescence relative humidity, DRH. The RH where the particle recrystallizes is the efflorescence relative humidity, ERH. The intermediate phases depend on the RH history of the particle. Figure from Beaver thesis (2008).

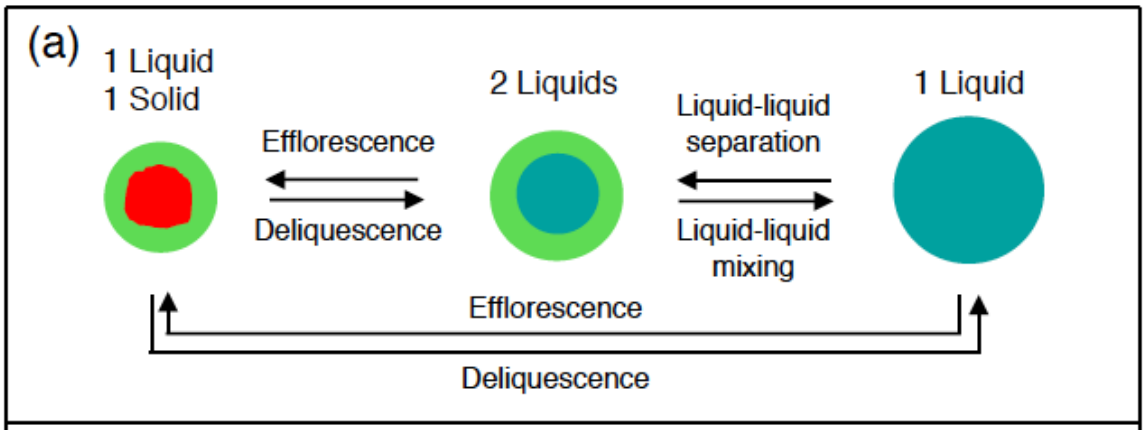

Figure 1.6 Possible phase transitions of mixed organic-ammonium sulfate particles. These transitions can occur as the RH in the atmosphere oscillates. The different colors represent different compounds and phases. Red is the crystalline ammonium sulfate, green is liquid organic, and aqua is an aqueous phase. Figure from Bertram et al. (2011).

compounds. Thus, LLPS may be a relatively common occurrence in the atmosphere, particularly with particles containing AS and a range of organics. More studies focusing on LLPS are needed to determine if phase separation can influence the RH at which particles deliquesce and effloresce.

1.4 Water Uptake Ability and Particle Phase

The phase of a particle directly affects how the particle takes up water. Figure 1.7 shows the particle growth as a function of RH of (a) a liquid, (b) a crystalline solid, and (c) an amorphous solid from Koop et al. (*Koop et al*., 2011). For a pure liquid (a), as the RH is increased the particle absorbs water until thermodynamic equilibrium is reached. More and more water is absorbed as the RH is increased to 100%. As the RH is decreased, the process follows the same curve because at every RH the thermodynamic equilibrium is independent of the pathway; there is not particle hysteresis. For a crystalline solid (b), as RH is increased, the solid is stable until an RH is reached at which the particle begins to take up water, DRH. From that point, the particle will continue to take up more water as the RH is increased. As the RH is decreased, the particle releases water, but as the RH falls below the DRH, a nucleation step is needed to release all the water from the particle. The RH continues to decrease, the particle becomes supersaturated and eventually nucleation occurs and the water is released at the ERH. At this point, the particle is a dry crystal in a stable state. In principle, the water uptake of an amorphous solid (c) should be the same as for a liquid; as the RH is increased the particle absorbs water until thermodynamic equilibrium is reached and then the particle continues to absorb more water. But, with an amorphous solid the equilibrium time scale is so long, the particle takes up water only on the outer monolayers. As the RH is increased, more and more

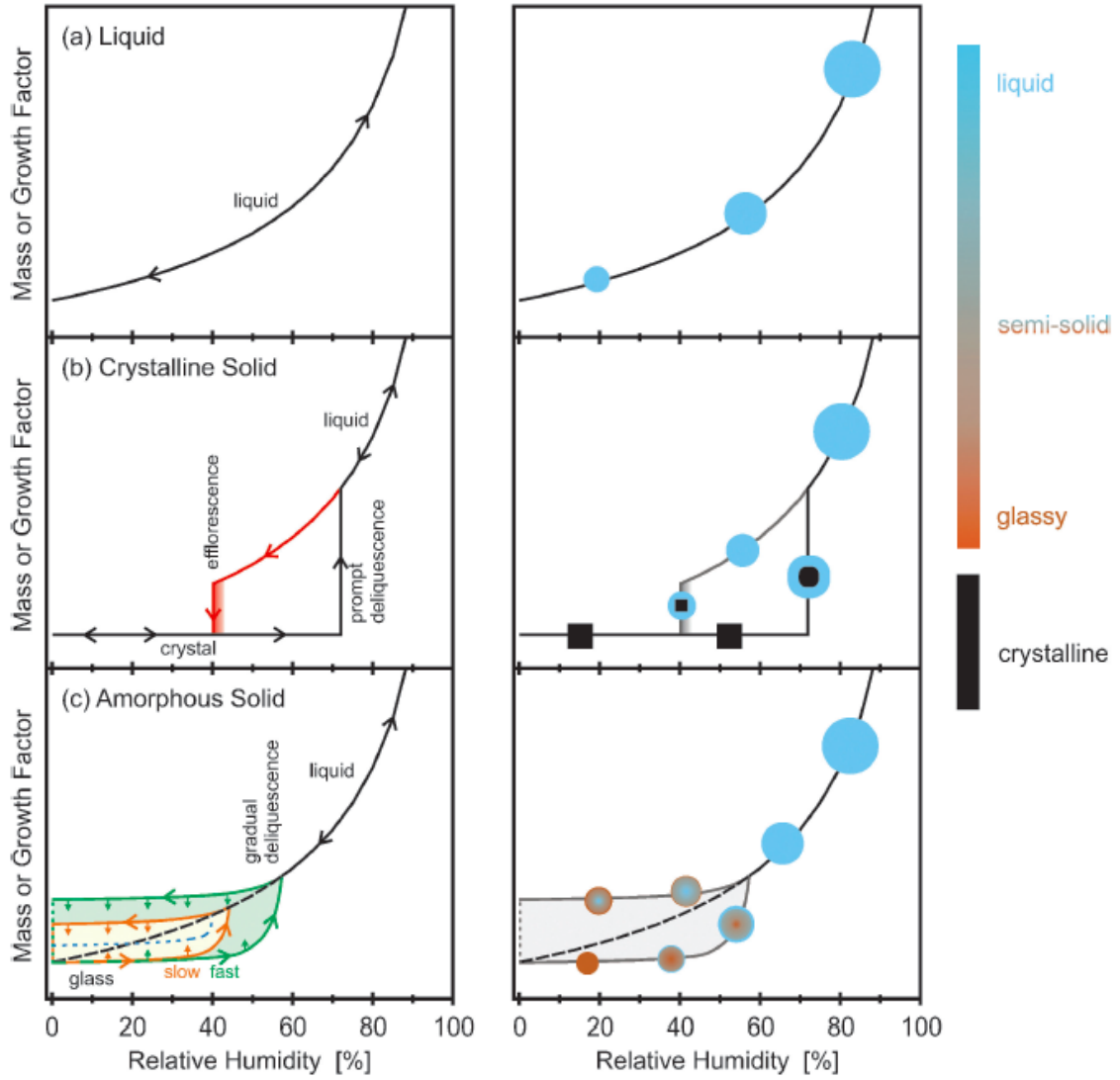

Figure 1.7 Water uptake behavior of aerosol particles (a) for a liquid particle, (b) for a crystalline particle, and (c) for an amorphous (semi-) solid. Figure from Koop et al. (2011).

layers take up water, inducing a self-accelerating process and a gradual deliquescence until the particle becomes a viscous liquid. This is termed a humidity-induced phase transition. It is important to understand the water uptake process for particles that are mixtures of crystalline solids, such as AS, and glassy organics, such as sucrose and raffinose.

1.5 Particle Light Extinction

Aerosol particles' interaction with incoming solar radiation can affect the climate. The attenuation of light can be described by the Beer-Lambert Law shown below in equation 1.1:

$$\frac{I}{I_0} = \exp\left(-\sigma_e l \right) \tag{1.1}$$

where I is the amount of light transmitted through the atmosphere, I_0 is the incident light intensity from the sun, σ_e (units of length^{-1}) is the extinction coefficient, and l (units of length) is the pathlength of the light. Both gases and particles affect light extinction, so σ_e is the sum of gas and particle absorption and scattering.

Incoming solar radiation has a broad wavelength range, with gases scattering light according to Raleigh scattering, while submicrometer particles scatter light in the Mie region. Mie scattering occurs when the particle diameter is similar to the wavelength of the incoming radiation and is the regime studied here. In Mie scattering, the particle extinction is a function of the wavelength of the incident radiation (λ), the number of particles (N), the particle diameter (D), and the real and imaginary parts of the refractive index (n and k).

The particle extinction will change as the RH changes, because the particle will take up and release water. The RH affects particle diameter, particle morphology, and refractive index through changes in particle hygroscopic growth. Therefore, to correctly calculate light extinction due to atmospheric particles, it is important to understand the particle chemical, physical and optical properties, including water content.

1.6 Thesis Focus

This thesis focuses on the investigation hygroscopic of optical growth of mixed organic and ammonium sulfate particles. Through laboratory experiments using cavity ring-down aerosol extinction spectroscopy we aim to better understand how particle size, chemical composition, and morphology affect aerosol optical properties. Chapter II explores how liquid-liquid phase-separated particles affect the water uptake ability of ammonium sulfate particles. Chapter III investigates the hygroscopic growth of mixed ammonium sulfate and amorphous solid particles and compares our data to models using the growth factor calculated for the mixtures in this study. General conclusions and future directions are given in Chapter IV.

Chapter II

Impact of Organic Coating on Optical Growth of Ammonium Sulfate Particles

2.1 Introduction

The direct and indirect effect of aerosols on the Earth's radiative balance remains one of the largest uncertainties in climate change (*Forster*, 2007). Aerosols directly interact with light by scattering and absorbing incoming solar radiation. Light extinction is the sum of scattering and absorption, and depends on both the chemical and physical properties of the particle. Ambient relative humidity (RH) also affects particle extinction because of changes in refractive index and particle size due to hygroscopic growth. To accurately include particles in radiative transfer models, knowledge of hygroscopic growth of relevant particle compositions is needed.

The composition of atmospheric aerosols is very complex and there is a large contribution from organic compounds (*Jimenez et al*., 2009). In ambient aerosols, there are often both inorganic and organic compounds found within the same particle (*Murphy et al*., 2006; *Pratt and Prather*, 2010). Ammonium sulfate (AS) is considered one of the most important inorganic salts found in submicron mixed particles (*Finlayson-Pitts*, 2000; *Seinfeld*, 2006). While the hygroscopic behavior of AS has been well characterized, there is still uncertainty in the water uptake behavior of mixtures of AS with various classes of organics (*Cziczo et al*., 1997; *Martin*, 2000). In addition to the amount of organic mixed in an AS particle, there may also be different morphologies within the particle. Past work has shown that particles containing AS and organics can become phase-separated and take on either core-shell or partially engulfed morphologies (*Bertram et al*., 2011; *Ciobanu et al*., 2009; *Marcolli and Krieger*, 2006; *Reid et*

al., 2011). To the authors' knowledge, the light extinction by such particles has not yet been studied.

As the RH of particles in a moving air mass oscillates and the temperature in the atmosphere fluctuates, mixed organic-ammonium sulfate particles can undergo LLPS, efflorescence, and deliquescence (*Bertram et al*., 2011; *Brooks et al*., 2002; *Ciobanu et al*., 2009; *Clegg et al*., 2001; *Erdakos et al*., 2006; *Krieger et al*., 2012; *Marcolli and Krieger*, 2006; *Martin*, 2000; *Pankow*, 2003; *Parsons et al*., 2004; *Smith et al*., 2011; *Song et al*., 2012; *Zuend et al*., 2010). The deliquescence RH (DRH) is the point at which a solid substance transforms into a liquid aqueous solution (*Mikhailov et al*., 2009). The efflorescence RH (ERH) is the RH at which a substance transforms from an aqueous solution into a solid. Because efflorescence requires nucleation, there is a hysteresis effect and the ERH is often well below the DRH. It has been shown in laboratory and modeling experiments that LLPS likely occurs in many atmospheric particles at RH values between the DRH and ERH (*Bertram et al*., 2011; *Chang and Pankow*, 2006; *Ciobanu et al*., 2009; *Clegg et al*., 2001; *Erdakos and Pankow*, 2004; *Marcolli and Krieger*, 2006; *Smith et al*., 2011; *Song et al*., 2012; *You et al*., 2012; *Zuend et al*., 2010). Previous laboratory experiments explored the relationship between LLPS and the O:C of the particle by probing particles deposited on a substrate using optical microscopy. Measurements showed that in multiple inorganic and organic mixtures, LLPS was observed in particles with O:C < 0.7. In contrast, particles with O:C > 0.7 did not undergo LLPS (*Bertram et al*., 2011). Another recent study collected atmospheric particle filter samples and measured the O:C of the water soluble fraction, finding O:C ~ 0.5 (*You et al*., 2012). Using optical and fluorescence microscopy on the water soluble filter particles, LLPS was observed while varying the RH (*You*

et al., 2012). Thus, LLPS may be a relatively common occurrence in the atmosphere, particularly with particles containing AS and a range of organics.

Most of the previous studies exploring LLPS use experimental techniques where droplets are in contact with a surface. Also, while much of the past work has determined the conditions at which LLPS will occur, there are fewer studies that explore the hygroscopic growth or change in optical properties. One study explored the hygroscopicity of mixed sodium chloride and oleic acid droplets using optical tweezers over a range of RH (*Dennis-Smither et al*., 2012). In that work, it was determined that the oleic acid only partially engulfed the NaCl core and that the organic did not affect the ERH or the DRH of the NaCl.

In the present work, we investigate hygroscopic optical growth from water uptake of liquid-liquid phase separated particles at varying RH. The optical growths of pure organic and inorganic particles are measured for comparison. Experimental results are compared to a model created for the expected optical growth assuming a homogeneous mixture and a core-shell structure.

2.2 Experimental Methods

Cavity ring-down aerosol extinction spectroscopy (CRD-AES) was used to determine the dependence of aerosol extinction on RH at 532 nm. The instrument used, shown in Figure 2.1, has previously been described in detail, so only a brief description will be provided here (*Baynard et al*., 2006; *Baynard et al*., 2007; *Beaver et al*., 2008; *Garland et al*., 2007). Slight modifications have been made and are described in detail.

Particles were generated using a syringe pump (Harvard Apparatus Model 70-2208) to inject aqueous AS and 1,2,6-hexanetriol solution into an atomizer (TSI 3076) with pre-purified

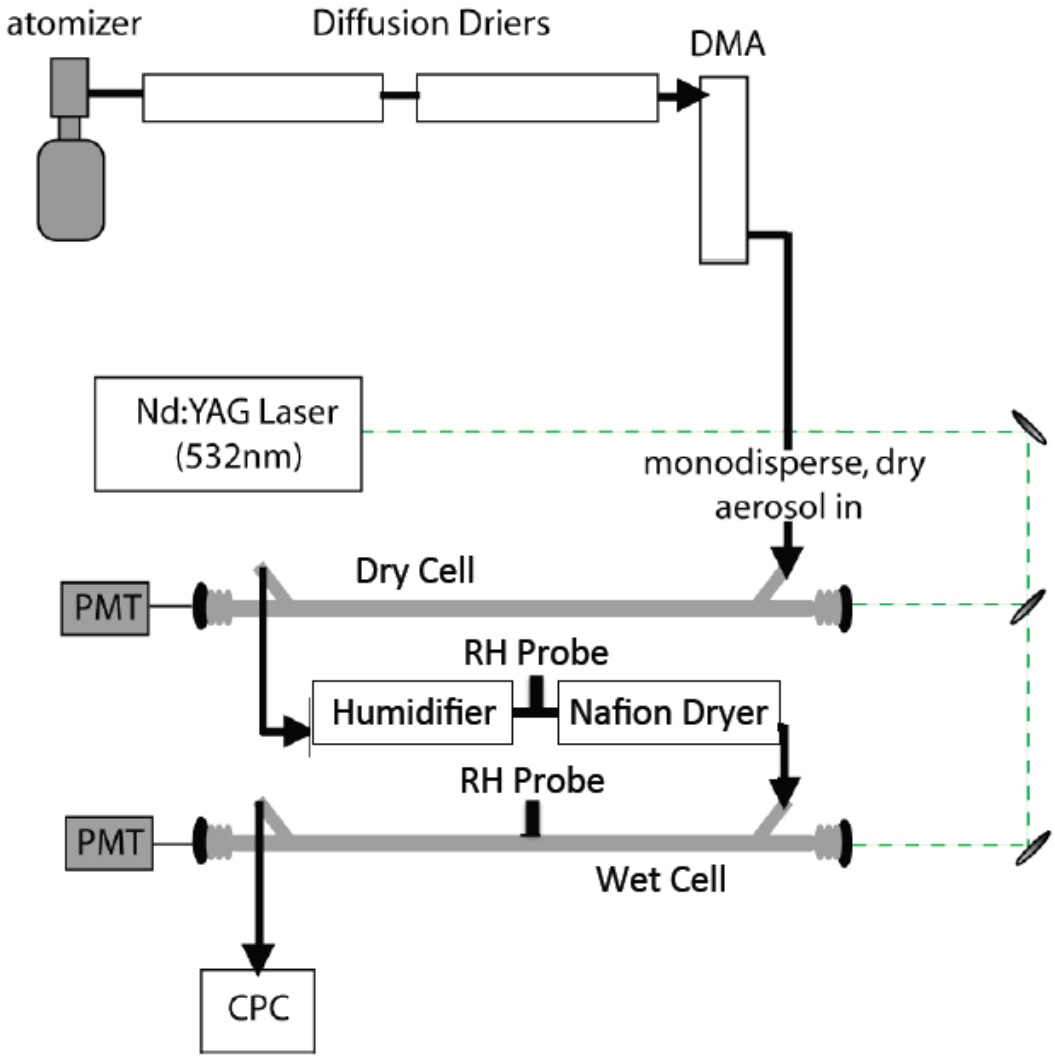

Figure 2.1 Schematic of the experimental set-up used for particle generation and to measure extinction.

N_2 as the carrier gas. After atomization, the particles were dried through two flask driers and two diffusion driers (TSI 3062). The drying system removed water and reduced the RH to <10%. After drying, the polydisperse particles entered a differential mobility analyzer (DMA, TSI model 3081). Particles were size selected to diameters from 200 - 500 nm. Size selection was performed with an atomized aerosol flow of 1.5 LPM and a sheath flow of 5.0 LPM.

The monodisperse flow from the DMA entered the first cell of the CRD-AES, where the extinction of the dry aerosol, b_{ext}(dry) Mm^{-1}, was calculated from the equation:

$$b_{ext}\ (Mm^{-1}) = \frac{R_L}{c}\ \left(\frac{1}{\tau} - \frac{1}{\tau_0}\right) \tag{2.1}$$

where c is the speed of light (m/sec), R_L is the ratio of the whole cavity length to the length that the aerosol sample occupies, τ_0 (sec) is the decay time measured when there are no particles present in the cavity, and τ (sec) is the decay time when there are aerosols present. Upon exiting the first cell, two different experiments were performed. The first experiment, "RH down", shown schematically in Figure 2.2a, was designed to study particles that had undergone LLPS. In this mode, the particles flowed into a temperature controlled humidification cell where they were exposed to RH between 80 – 90%, causing deliquescence. The humidification cell is a stainless steel tube containing a water vapor-permeable membrane surrounded by liquid water and held at 30°C. Humidification of the particles is necessary to achieve LLPS, because the particles must reach deliquescence before LLPS can occur. After humidification, the particles flowed into a Nafion drier (Accurel, Permapure). The addition of the Nafion drier is a modification made to the previously described experimental set-up. The Nafion dryer also has a water permeable membrane, but with a pre-purified nitrogen sheath flow surrounding the aerosol

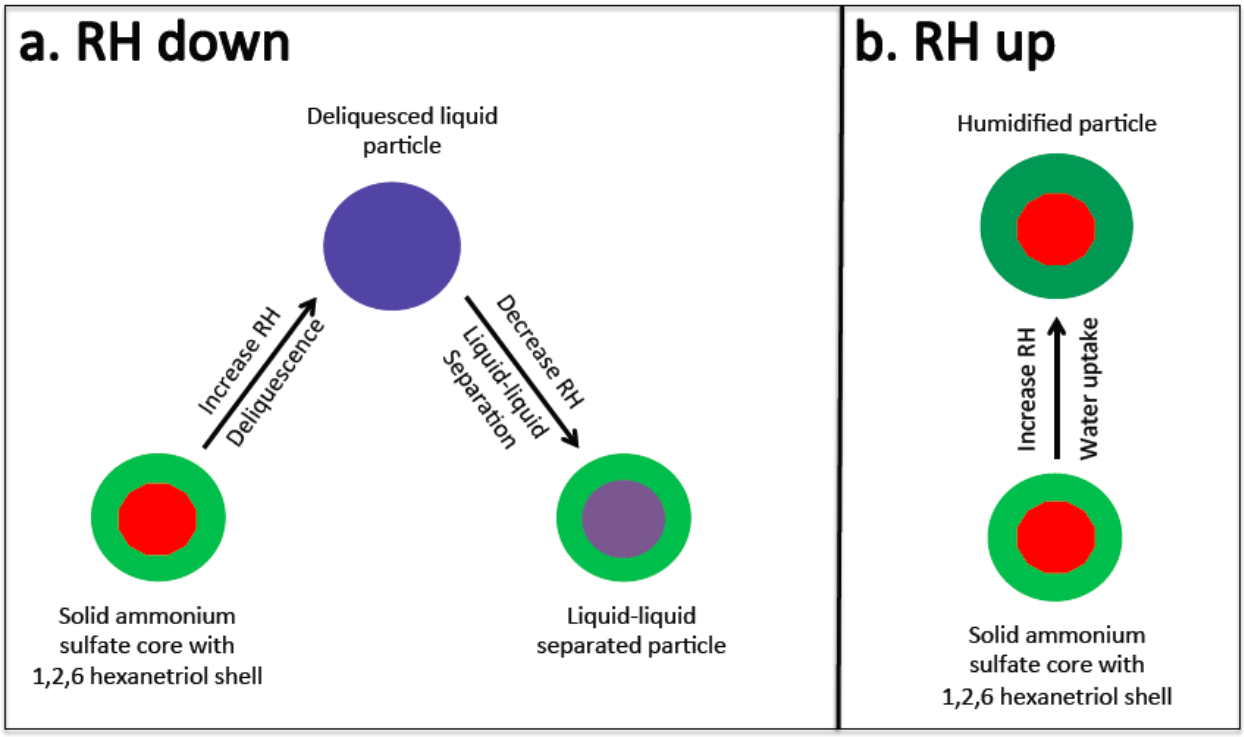

Figure 2.2 Schematic of the two experiments performed. Process (a.) begins with dry atomized particles whose relative humidity is increased until deliquescence, and then decreased to form a liquid-liquid separated particle. Process (b.) begins with dry atomized particles whose relative humidity is increased, but remains below the deliquescence relative humidity.

flow within the tube. The membrane absorbs water from the liquid particles and evaporates it into the sheath flow. With the sheath flow varied between 0.1 – 4 LPM, the particles are partially dried to an RH between 46 – 65%. Following the Nafion drier, the humidified particles flowed into a second CRD-AES cell where the wet extinction, b_{ext}(wet) Mm^{-1}, were measured at an elevated RH. The RH and temperature were monitored with Vaisala Humitter 50Yprobes (±3% accuracy) between the humidification cell and the Nafion drier and within the second CRD-AES cell. Finally, the particles exited the CRD-AES and flowed into a condensation particle counter (CPC, TSI 3775).

In the second type of experiment, "RH up" (Figure 2.2b), after exiting the first CRD cell, the particles entered the humidification cell where they are exposed to RH between 46 – 80%. The particles then flowed into the second CRD cell where the wet extinction and RH were measured. The particles exited the CRD and flowed into a CPC where the number concentration (particles/cm^3) was measured.

The ratio of the humidified extinction to the dry extinction from the cells is defined as the optical growth factor fRH_{ext}(RH, dry):

$$fRH_{ext}(\text{RH, dry}) = \frac{b_{ext}(wet)}{b_{ext}(dry)} \tag{2.2}$$

and is used to describe the RH dependence of light extinction. Because the extinction is measured as a function of particle size, multiply charged particles from the DMA must be taken into account. To account for multiply charged particles, an optical effective diameter D_{eff} is used, as has been done in previous optical growth studies (*Beaver et al.*, 2008; *Garland et al.*, 2007; *Hasenkopf et al.*, 2011). To calculate D_{eff}, the number concentration, N (particles/cm^3), and the extinction, b_{ext} (Mm^{-1}), were used to determine the effective extinction cross-section, σ_{ext}

(cm^2) = b_{ext}/N, as a function of particle size. By using Mie theory and the refractive index (RI) of the individual compounds and the mixture, the theoretical calculated cross-sections were determined. The experimental extinction cross-sections were compared to the calculated cross-sections and the particle diameter where the experimental and calculated cross-sections were equal is the corresponding effective optical diameter, D_{eff}.

The RI of ammonium sulfate (n = 1.53, k = 0) and 1,2,6-hexanetriol (n = 1.478, k = 0) are both well known (*Aldrich Chemical Company*, 1996). However, the RI for the dry mixture was needed to determine D_{eff} for the mixed particles. It has previously been shown that measured refractive indices for a mixture do not necessarily agree with the volume-weighted average of the pure components (*Freedman et al*., 2009). Therefore, we measured the RI for the dry mixed particles studied here. The RI for the dry 2:1 (mass ratio) mixture of 1,2,6-hexanetriol and ammonium sulfate was determined using CRD-AES. This experimental procedure has previously been described, so only a brief description will be provided here (*Freedman et al*., 2009; *Zarzana et al*., 2012). The particles are created using the same atomizer and dryer set-up previously described in this work and the particles are sized selected by the DMA with the same aerosol and sheath flow. The particle flow enters the CRD-AES cell, where the extinction is measured. The particles then exit the CRD-AES and flow directly into a CPC. The RI for the mixture is determined using Mie scattering theory to compare the predicted extinction to the experimental extinction as a function of particle size (*Freedman et al*., 2009; *Zarzana et al*., 2012).

In a separate experiment, the morphologies of the mixed particles with the same overall composition as those in the CRD experiments were probed using optical and Raman microscopy. The experimental setup to obtain both optical images and Raman line maps of a 2:1 mixture of

1,2,6-hexanetriol and ammonium sulfate has been previously described in detail (*K. J. Baustian et al.*, 2010; *Schill and Tolbert*, 2012). A Nicolet Almega XR Raman microscope has been equipped with a Linkham THMS600 environmental cell and Buck Research CR-1A chilled-mirror hygrometer. The spectrometer is also coupled to an Olympus BX51 research grade optical microscope with 10x, 20x, 50x, and 100x capabilities. Particles were generated by aspirating a solution of 2% 1,2,6-hexanetriol and 1% ammonium sulfate by weight using a Meinhard TR-50 glass concentric nebulizer onto a hydrophobically treated quartz disc. The resulting particles range from 1-40 μm in lateral diameter.

Three systems were studied in this work: aqueous solutions of ammonium sulfate (Fisher Scientific, Certified ACS, granular), 1,2,6-hexanetriol (Sigma-Aldrich, 96%), and a 2:1 (mass ratio) 1,2,6-hexanetriol:ammonium sulfate mixture. All solutions were prepared using HPLC grade water and total solution concentrations were between 1.5-3.0 wt%. The total concentrations were kept low to reduce the interference of doubly charged particles.

2.3 Results and Discussion

2.3.1 Particle Characterization with Raman and Optical Microscopy

Particle optical growth was measured for freely flowing submicron sized particles using the CRD-AES. To verify that the particles seen in the CRD would form core-shell particles, additional experiments were performed on larger particles deposited on a substrate, but subjected to the same RH conditions. Figure 2.3 shows optical images and Raman line maps of a single particle during a cycle starting at 0% RH, increasing the RH to 90%, and finally decreasing the RH to 61%, all at 290 K; these are the same steps described in Figure 1a. Raman line maps were taken through the center of each particle as a horizontal line. For each line map, a Raman

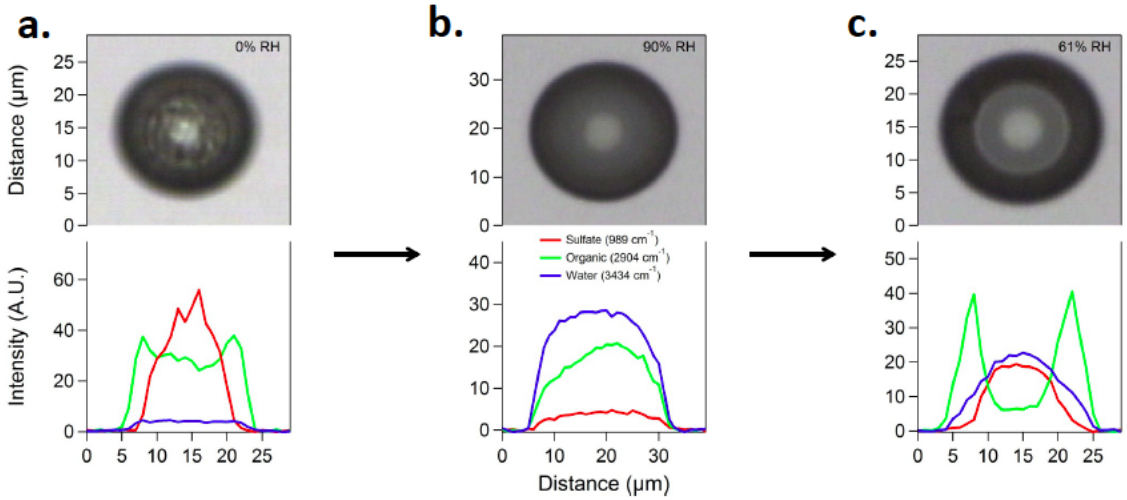

Figure 2.3 Optical images and Raman line maps for (a.) a dry mixture particle of ammonium sulfate and 1,2,6 hexanetriol, (b.) the same particle deliquesced, and (c.) the same particles in LLPS.

spectrum was taken every 1-micrometer across the particle. From each map, the height of three peaks is plotted as a function of distance. These peaks correlate to presence of ammonium sulfate (sulfate stretch, 989 cm^{-1}), 1,2,6-hexanetriol (C-H stretch, 2904 cm^{-1}), and water (O-H stretch, 3434 cm^{-1}). As suggested in Figure 1a, the particle initially assumes an ammonium sulfate core, organic shell morphology at 0% RH. Visually, the AS center of the particles appear crystalline. The Raman spectra show there is no water peak, as expected for an effloresced inorganic salt with a liquid organic coating at 0% RH. There is a small increase in intensity at 3434 cm^{-1} that coincides with the AS sulfate signature; however, this is due to the shoulder of the N-H stretch of the ammonium ion. An organic coating is clearly evident in the Raman line map at 0% RH. At 90% RH, the particle is a homogeneous aqueous solution. This is most clear in the Raman line map, where all three components have a similar distribution. After lowering the RH to 61% RH, the particle has undergone LLPS. This is seen visually, because there is a clear separation in the two components. Raman line maps also show the organic is concentrated at the far ends of the particle and the sulfate core is in the center. Water is mostly associated with the AS core. While we are not able to image the freely-floating submicron particles, we assume aqueous core-liquid organic shell morphology for the LLPS particles. We cannot, however, rule out partially engulfed structures for the free-floating particles.

2.3.2 Refractive Index Determination

The refractive index for the mixed, dry 1,2,6-hexanetriol and ammonium sulfate particles was determined by comparing the measured and calculated dry extinction, b_{ext}(dry) (cm^{-1}). The calculated dry extinction measured by the CRD is given by

$$b_{ext} = \frac{CQ_{ext}(n,k,D,\lambda)\pi D^2}{4} \quad (2.3)$$

where C is the concentration (cm^{-3}), Q_{ext} is the extinction efficiency, and D is the particle diameter (cm). Q_{ext} is dimensionless and depends on the real and imaginary parts of the refractive index, the wavelength of incident light, and the particle diameter. Using this equation and varying the refractive index, the best fit can be found to the measured extinction. Our group's method for retrieving the real and imaginary parts of the refractive index have previously been described and validated (*Freedman et al*., 2009; *Hasenkopf et al*., 2010; *Zarzana et al*., 2012).

In Figure 2.4, the measured and calculated extinction efficiencies are shown as a function of particle diameter for our best fit refractive index. The measured values have been corrected for doubly charged particles. The measured and calculated extinction efficiency values agree reasonably well. The best-fit refractive index was determined to be n = 1.49, k = 0 for the mixture. The measured refractive index differs only slightly from the volume-weighted average of the pure components calculated as:

$$n_{dry} = \frac{V_{AS}n_{AS} + V_{HT}n_{HT}}{V_{AS} + V_{HT}} \quad (2.4)$$

where AS = ammonium sulfate and HT = 1,2,6-hexanetriol and V represents volume. The calculated refractive index using equation (4) is n = 1.51, k = 0. In contrast to a previous study of mixtures of dicarboxylic acids with AS, the volume-weighted and measured refractive index agree quite well in the present case (*Freedman et al*., 2009).

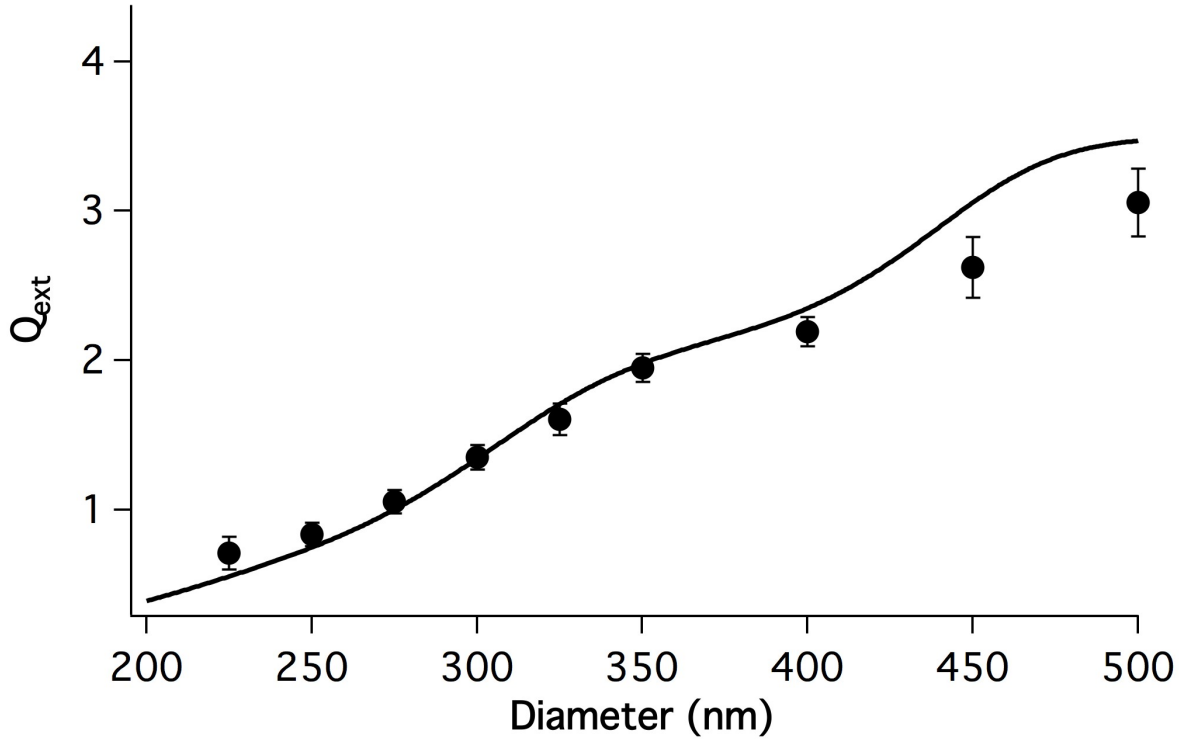

Figure 2.4 The measured Q_{ext} values (black circles) and calculated Q_{ext} values (solid line) using the best fit refractive index for dry 2:1 mixture of 1,2,6-hexanetriol and ammonium sulfate at room temperature.

2.3.3 Aerosol Optical Growth

The optical growth in the RH down mode, $f\mathrm{RH}_{ext}$, results for pure AS at RH = 46%, 65%, and 80% as a function of particle size are shown in Figure 2.5. The data were compared to theoretical predictions calculated from the extended Aerosol Inorganic Model (e-AIM) and Mie Theory (*Clegg et al.*, 1992; *Clegg et al.*, 1998; *Wexler and Clegg*, 2002). The e-AIM is a thermodynamic model that calculates partitioning of water between the gas and liquid phases based on the relative humidity, temperature, and chemical composition. With the e-AIM model, for each of the three RHs shown, the mass of water that was taken up at each size was calculated. Using the bulk densities of water (1.0 g/cm^3) and AS (1.77 g/cm^3), the volume of each was calculated and used to determine both the size of the AS/water particle, as well as the volume-weighted refractive index. The extinction due to the wet and dry particles was then calculated and used to determine the theoretical $f\mathrm{RH}_{ext}$ plotted as lines in Figure 2.5. As the RH decreases, less water is taken up by the particles and the $f\mathrm{RH}_{ext}$ decreases as RH decreases. Optical growth is seen at every RH with the RH down procedure because the particles have been deliquesced, but not effloresced (*Martin*, 2000). The data agree reasonably well with the corresponding e-AIM model calculations. The e-AIM model shows small oscillations with particle size that are not seen in our data. This is because in our experiment there is a distribution of particles sizes around the mean. In addition, the presence of multiply charged particles tends to wash out the oscillations. Experiments were also performed at 65% RH for RH up (not shown). In this case, there was no water uptake observed within error because the particles were not deliquesced.

Because 1,2,6-hexanetriol is not included in the e-AIM model, it wasn't possible to compare the optical growth with theoretical predictions. Instead, we use data to determine growth factors of 1,2,6-hexanetriol. The calculated hygroscopic growth factor values for pure

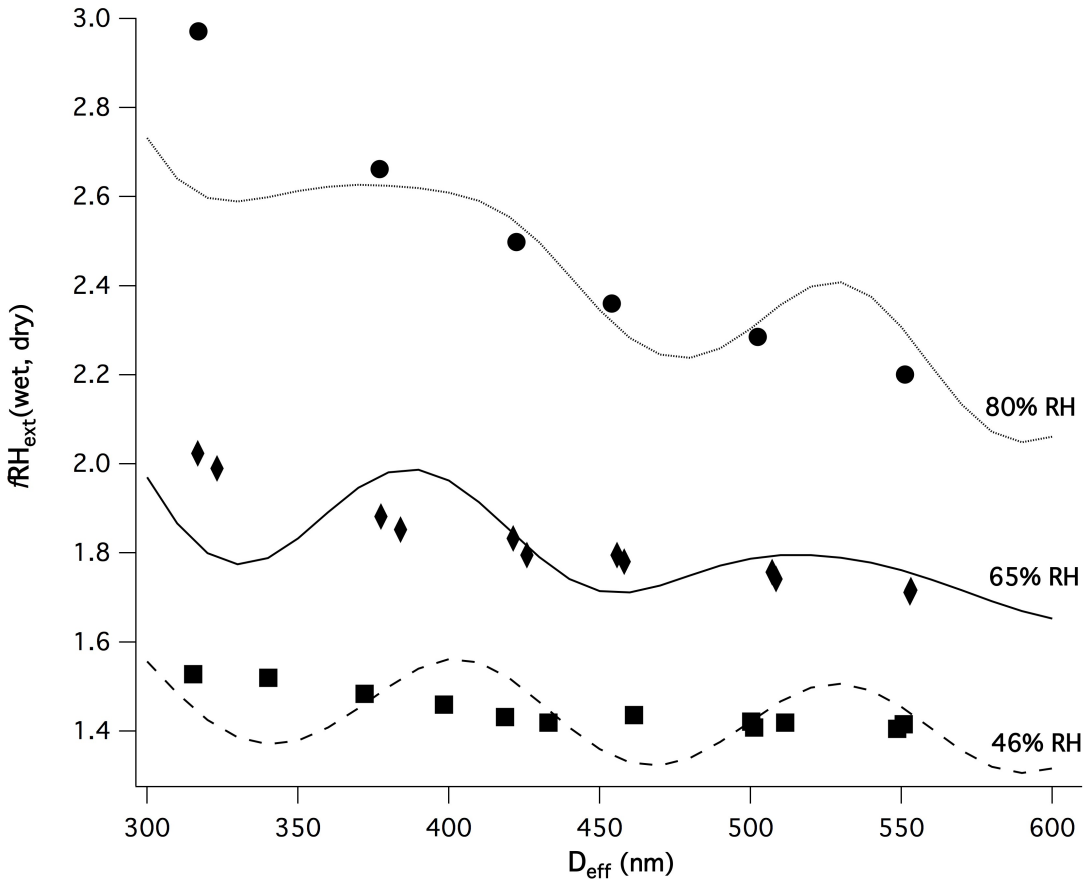

Figure 2.5 $f\mathrm{RH}_{ext}$, RH down, for ammonium sulfate at RH = 80% (circles), 65% (diamonds), and 46% (squares) for a range of particle diameters. The lines represent predicted $f\mathrm{RH}_{ext}$ values for ammonium sulfate using e-AIM and Mie Theory.

1,2,6-hexanetriol are shown in Figure 2.6. The growth factor is plotted as a function of particle size for the RH up data at 47%, 65%, 80% and 88% RH. Hygroscopic growth factor (Gf), or physical growth, is defined as the wet particle diameter divided by the dry particle diameter at a specific RH, $Gf = D_{wet} / D_{dry}$. Mie theory was used to calculate Gf from the measured $f\mathrm{RH}_{ext}$. To calculate the physical growth, the extinction was calculated for particles whose diameter ranged from the dry diameter to 2.25 times the dry diameter. The water volume needed to cause this change in size was determined, and used to calculate the RI of the wet particles. The refractive index and size was then used to calculate an $f\mathrm{RH}_{ext}$ value for each growth factor. The calculated $f\mathrm{RH}_{ext}$ values were compared to the experimental $f\mathrm{RH}_{ext}$ values, and the diameter with the best match was used to determine the physical growth (*Hasenkopf et al*., 2011). As the RH increases, the hygroscopic growth factor increases. Because 1,2,6-hexanetriol is liquid at room temperature, there is water uptake for all the RH up and down experiments, even at low RH, unlike ammonium sulfate. The dashed lines are the averaged Gf at each RH. The $f\mathrm{RH}_{ext}$ and Gf data were collected for the same RH range, 47%, 65%, and 80% using the RH down experimental set-up. The two different experimental set-ups yielded very similar results at each RH. This indicates that there is not a hysteresis effect for 1,2,6-hexanetriol. Although the 1,2,6-hexanetriol takes up more water than AS before deliquescence as the RH increases, as RH decreases, there will be much more water uptake in a pure AS particle than in a pure 1,2,6-hexanetriol particle for the same size particle.

A 2:1 organic and AS mixture was also studied at multiple particle sizes for varying RH. In Figure 2.7, as the RH is increased (RH up), there is slight optical growth at each RH, consistent with the 1,2,6-hexanetriol taking up water. The solid black line shows the exponential

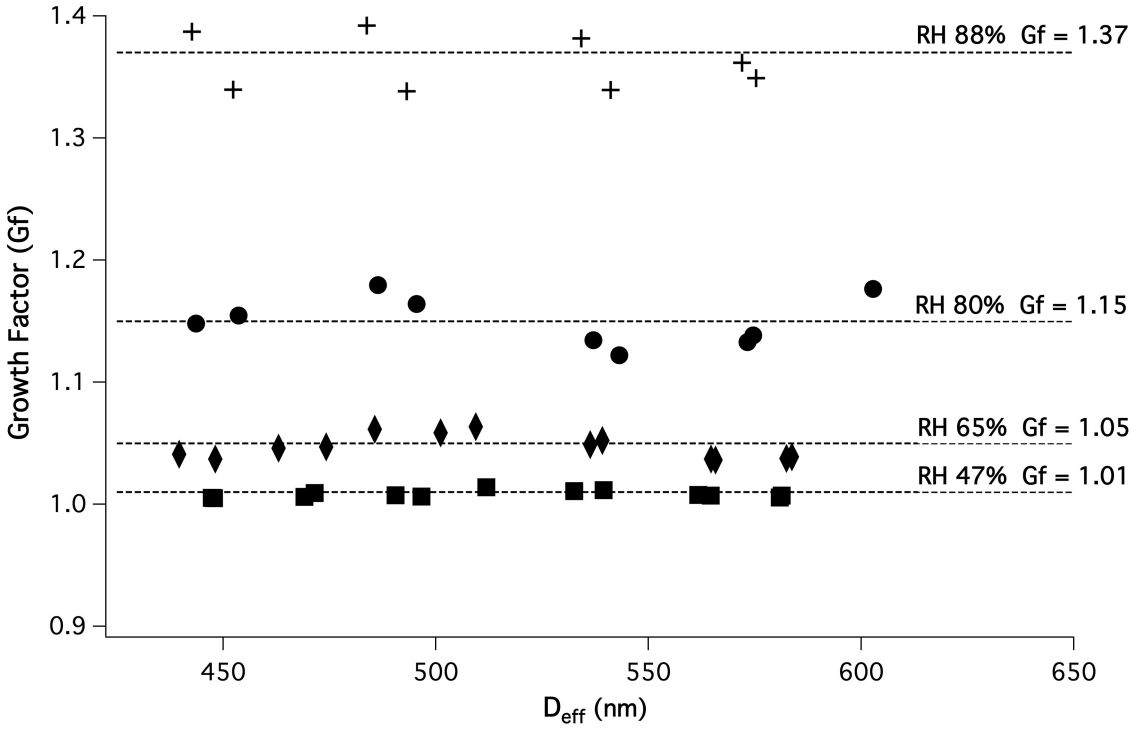

Figure 2.6 Growth factor (Gf) for pure 1,2,6-hexanetriol versus the effective diameter at RH = 88% (plus sign), 80% (circles), 65% (diamonds), and 47% (squares). The lines represent the average Gf for each RH.

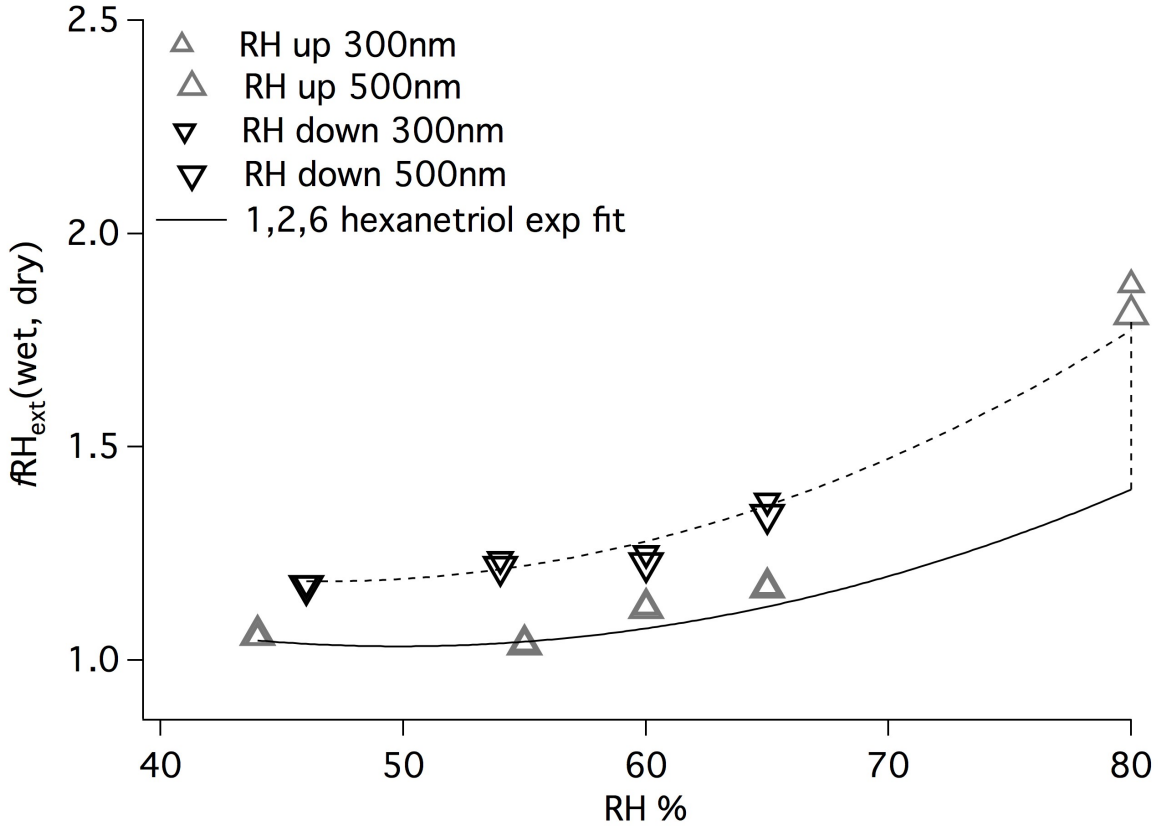

Figure 2.7 $f\mathrm{RH}_{ext}$ of 2:1 1,2,6-hexanetriol:AS mixed particles versus RH for RH up (upward facing triangles) and RH down (downward facing triangles) for 300 and 500 nm particles. The solid black line shows the exponential fit of all the 300 nm pure 1,2,6-hexanetriol data. The dashed line shows the hysteresis of the mixed particle.

fit of all the 300 nm pure 1,2,6-hexanetriol data to illustrate that increasing the RH for the mixture particles has similar water uptake as the pure 1,2,6-hexanetriol particles. The optical growth for RH up at 80% is much larger than the pure 1,2,6-hexanetriol, because both the ammonium sulfate and 1,2,6-hexanetriol can take up water because as the particles are above the ammonium sulfate DRH (*Bertram et al*., 2011). As the RH is decreased there is also water uptake at each RH. The dashed line (to guide the eye) shows the hysteresis effect observed for the mixed particles. In this case, there is water uptake in the ammonium sulfate part of the particles because the particles have deliquesced and are above the ammonium sulfate ERH.

Figure 2.8 shows $f\mathrm{RH}_{\mathrm{ext}}$ (dry, 80%) for pure ammonium sulfate, pure 1,2,6-hexanetriol, and 2:1 mixture data as a function of particle size. Under these conditions, the AS should be deliquesced and we expect the particle to be a homogeneous mixture of AS, 1,2,6-hexanetriol, and water as shown in Figure 2.2b. It can be seen that the mixed particle data exhibit $f\mathrm{RH}_{\mathrm{ext}}$ values between the pure ammonium sulfate data and the pure 1,2,6-hexanetriol data. Further, $f\mathrm{RH}_{\mathrm{ext}}$ values are similar as the RH is both increased and decreased. This result was expected because at 80% RH the 2:1 mixture particles are fully deliquesced.

Three theoretical models were used to simulate the optical growth for the mixture at 80% RH. The first model (solid gray line) assumes that the organic and inorganic are homogeneously mixed, but that only ammonium sulfate is taking up water. The volume of the both AS and 1,2,6-hexanetriol fractions of the particle were determined using the given particle diameter and the mass weight % of each component used in the 2:1 mixture experiments. The water volume taken up by the AS fraction of the particle was determined using the e-AIM model. There is not currently data in the e-AIM model for phase partitioning for the organic 1,2,6-hexanetriol, so water uptake of the organic could not be taken into account using e-AIM. The wet diameter was

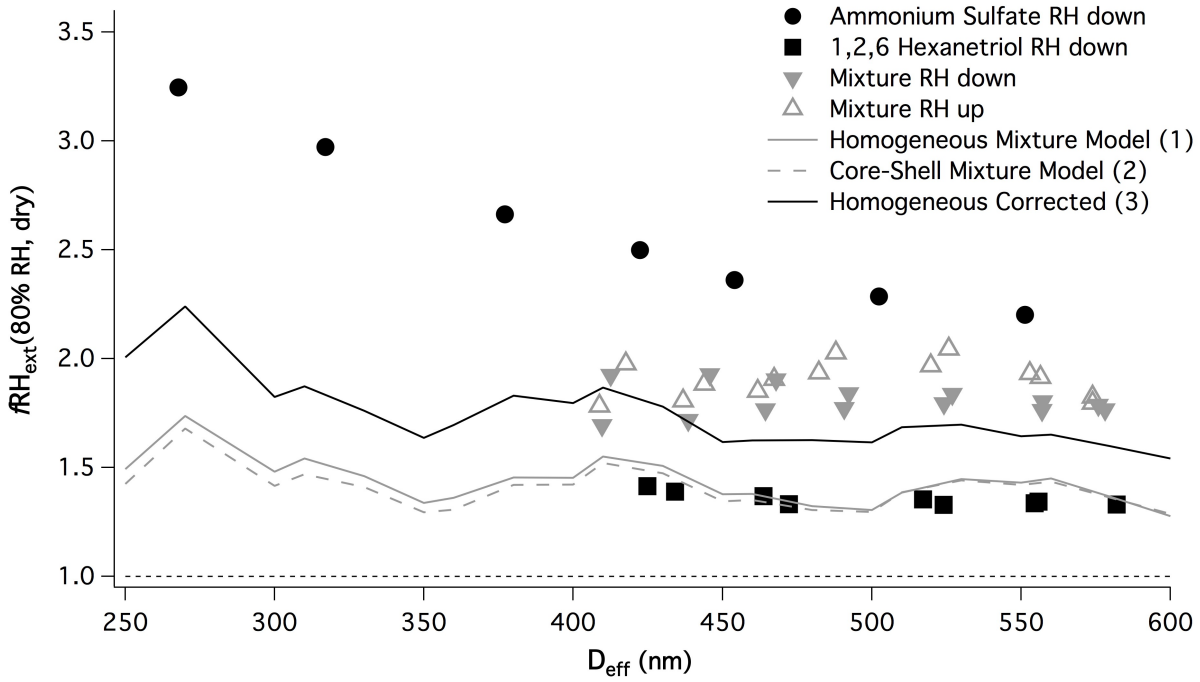

Figure 2.8 $f\mathrm{RH}_{ext}$ versus the effective diameter at RH = 80% for RH down experiment (solid symbols) and RH up experiment (open symbols). The solid gray line is the modeled *f*RH of the mixture assuming homogeneously mixed particles and the dashed gray line is the modeled *f*RH of the mixture assuming a core-shell structure. The solid black line is the modeled *f*RH of the mixture for homogeneously mixed particles including water uptake of pure 1,2,6 hexanetriol data.

determined by adding up the total particle volume (including the AS, 1,2,6-hexanetriol, and water fractions), assuming a spherical particle. The RI for the homogenous mixture, and size parameter were also needed to create the model. To determine the RI at each diameter, a volume weight RI was calculated:

$$n_{wet} = \frac{V_{AS}n_{AS} + V_{HT}n_{HT} + V_{H_2O}n_{H_2O}}{V_{AS} + V_{HT} + V_{H_2O}} \quad (2.5)$$

Each compound is non-absorbing, therefore k = 0. Mie codes were used to determine the theoretical extinction for both the wet and dry homogeneously mixed particles, values which were then used to calculate the $f\text{RH}_{\text{ext}}$. The second model (dashed gray line) assumes that the organic and inorganic components have undergone LLPS and are in a core-shell morphology, again with only the ammonium sulfate core allowed to take up water. The ammonium sulfate water uptake was again determined using the e-AIM model. To calculate the theoretical $f\text{RH}_{\text{ext}}$, an algorithm based on Mie Theory for particles with core-shell morphology was used to determine the theoretical extinction, b_{ext} (Mm^{-1}), for both the wet and dry core-shell particles and then used to calculate the $f\text{RH}_{\text{ext}}$ (*Bohren and Huffman*, 1983). The RI for both ammonium sulfate and 1,2,6-hexanetriol are used in the algorithm. It can be seen that the first and second models both show a similar optical growth for each particle size. The similarities of the models stem from the fact that the RI for both the homogenous mixture and the LLPS particles were very similar. The volume weight RI for the homogenous mixture varied from 1.435 – 1.464 for multiple RH%, and the RI's for pure ammonium sulfate and pure 1,2,6-hexanetriol were 1.53 and 1.478, respectively. However, neither the first or second model agrees with the mixture data

because the 1,2,6-hexanetriol is almost constantly taking up water, which is not accounted for in either model.

A third model (solid black line, labeled Homogeneous Corrected) assumes the same homogeneous mixture as the first, but since the 1,2,6-hexanetriol partitioning data are not available in the e-AIM model, the pure 1,2,6-hexanetriol water uptake data from this study were used. The volumes of the AS, 1,2,6-hexanetriol, and water from AS uptake were calculated as in the first model. To calculate the water volume added from 1,2,6-hexanetriol taking up water, the Gf of pure 1,2,6-hexanetriol was used to calculate the wet particle volumes at RH = 53% and 80% for particles ranging in size from 200-600 nm. The total mixed particle volume for each particle size was then calculated by added the dry ammonium sulfate volume, the dry 1,2,6-hexanetriol volume, the water volume taken up by the ammonium sulfate, and the water volume taken up by the 1,2,6-hexanetriol. From the total particle volume the wet particle diameter was calculated, assuming the particle is spherical. It can be seen that there is much better agreement with the third model and the mixture data once the 1,2,6-hexanetriol water uptake data are taken into account. Since the homogenous and core-shell models with only ammonium sulfate water uptake taken into account agree so well, it is likely that a core-shell model where 1,2,6-hexanetriol water uptake is incorporated, would agree well with the mixture data as well.

In contrast to the optical growth at RH = 80%, significant differences are observed in the mixed particles at RH = 53% depending on whether the RH is increased or decreased as shown in Figure 2.9. At RH = 53%, for the RH down mixture data the particles are observed to take up water at levels between the pure ammonium sulfate and pure 1,2,6-hexanetriol particles at each particle size. However, when RH is increased from low levels, there is very little water uptake observed. In fact, the mixed particles data as RH is increased are indistinguishable from pure

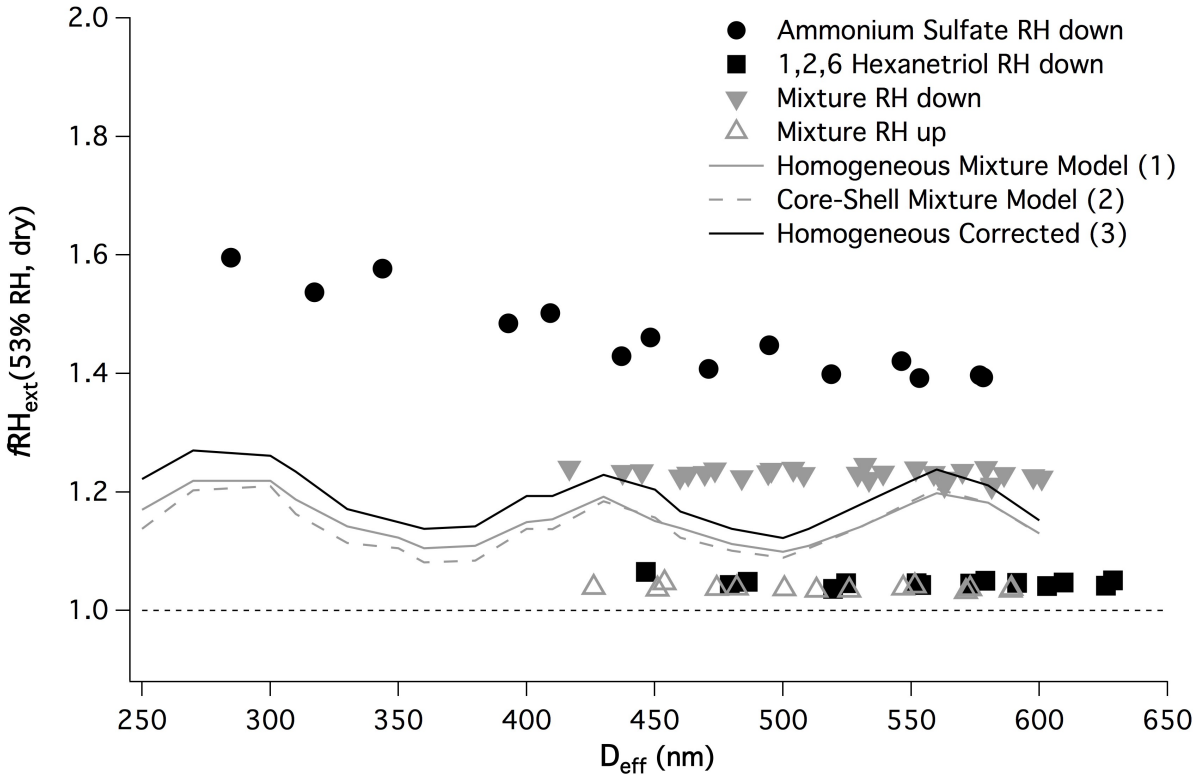

Figure 2.9 $f\mathrm{RH}_{\mathrm{ext}}$ versus the effective diameter at RH = 53% for RH down experiment (solid symbols) and RH up experiment (open symbols). The solid gray line is the modeled *f*RH of the mixture assuming homogeneously mixed particles and the dashed gray line is the modeled *f*RH of the mixture assuming a core-shell structure. The solid black line is the modeled *f*RH of the mixture for homogeneously mixed particles including water uptake of pure 1,2,6 hexanetriol data.

1,2,6-hexanetriol data. This suggests that at RH = 53%, if the particle was previously deliquesced (as in RH down), the ammonium sulfate is the dominant component taking up water. If the particle was instead dry (as in RH up), only a small amount of water is taken up by the organic. The same three models were used to calculate the water uptake for RH = 53%. The models only taking ammonium sulfate water uptake into account more closely agree with the mixture data at RH = 53% than at RH = 80%. This is due to the fact that there is less water uptake by the organic at lower RH. With the model including 1,2,6-hexanetriol water uptake, the data agree even more closely. Again, we do not see oscillations in the data. This is because in our experiment there is a distribution of particles sizes and we have multiply charged particles.

2.4 Conclusions and Implications

The main finding of this work is that the water uptake of a mixed LLPS particle depends on the RH history of an air parcel. It can also be concluded that at room temperature for LLPS mixed particles containing sulfates and organics similar to 1,2,6-hexanetriol:

1) If the AS is deliquesced, the mixed particle optical growth will be between pure ammonium sulfate and whatever organic it is mixed with. In this case, the *f*RH can be explained by mixing rules to first order approximations. Because the organic coating is liquid and water diffusion is rapid, particle morphology does not change the particle's ability to take up water.

2) For liquid organic coatings, the coating does not appear to inhibit AS and water lost in crystallization readily diffused to the core and evaporates. As RH is increased to RH = 53%, the growth of the mixed particles is very similar to the growth of the pure 1,2,6-hexanetriol particles. If the organic coating inhibited AS crystallization, there would be much more growth because both the AS and organic would take up water.

3) Overall, the water uptake behavior is dictated by the AS portion of the mixed particle, similar to the behavior seen in homogeneously mixed particles (*Beaver et al*., 2010; *Beaver et al*., 2008). A previous study has found a linear relationship between optical growth and the inorganic and organic content of the particle, following the Zdanovskii-Stokes-Robinson relationship (*Stokes and Robinson*, 1966). The relationship assumes that each component of the mixture acts independently, that no interaction between the components occurs, and that the optical growth is additive. This relationship seems to still hold true for the LLPS particles seen in this study when the AS is deliquesced.

4) For the systems where LLPS has occurred, the refractive indices for each component in the system may similar be to each other (*Bertram et al*., 2011). AS has a RI of 1.53, and the RI of the organic compounds where phase separation is observed range from 1.43 – 1.67 (*RSC*). The refractive index values for ammonium sulfate and 1,2,6-hexanetriol are also similar to each other. In this case, the core-shell model and homogeneous model gave similar results for optical growth. Therefore, for other LLPS systems, there may not be much difference between the optical growth of homogeneous mixtures and the core-shell morphologies observed in the LLPS mixtures.

While not studied in the present work, other areas where LLPS could influence atmospheric processes is in how the particles act as CCN and how they catalyze heterogeneous atmospheric reactions. Additional studies that test the influence of LLPS on particle chemical reactivity and ability to act as CCN would be highly desirable.

Chapter III

Optical Growth of Glassy Organics Sulfate Particles

3.1 Introduction

Atmospheric aerosols are important to understanding Earth's radiative balance. They affect climate directly by scattering and absorbing radiation, the sum of which is termed light extinction. Light extinction is dependent on particle size, composition, and morphology. Relative humidity (RH) can also affect light extinction by changing particle size due to hygroscopic particle growth. Laboratory studies of the hygroscopic growth of mixed composition aerosols are needed for inclusion into radiative transfer models.

Organic compounds make up a large fraction of atmospheric aerosols (*Jimenez et al.*, 2009). Although organics aerosols are abundant in the atmosphere, their composition, and chemical and physical properties are poorly understood. In addition, organic compounds are usually found to be mixed with inorganic compounds within a single particle (*Murphy et al.*, 2006; *Pratt and Prather*, 2010). Ammonium sulfate (AS) is the most abundant inorganic salt found in non-marine tropospheric aerosols (*Seinfeld*, 2006). While the hygroscopic behavior of AS has been well characterized, there is still uncertainty in the water uptake behavior of mixtures of AS with various classes of organics (*Cziczo et al.*, 1997; *Martin*, 2000). In particular, recent attention has focused on the possibility that organic glasses make up an important class of atmospheric particulates (*K. J. Baustian et al.*, 2012; *Koop et al.*, 2011; *Mikhailov et al.*, 2009;

Schill and Tolbert, 2012; *Zobrist et al*., 2008). It is unclear how organic glasses will impact hygroscopic growth when mixed with AS inorganic particles.

Glasses are non-crystalline amorphous solids that behave mechanically like solids, and experimentally defined as having a viscosity > 10^{12} Pa s (*Angell*, 1995; *Debenedetti and Stillinger*, 2001). For crystalline solids as RH is increased, there is prompt dissolution into solution at the deliquescence RH (DRH), and the phase change is well-characterized for common inorganic atmospheric aerosols (*Dai et al*., 1997; *Martin*, 2000; *Shindo et al*., 1997; *Tang and Munkelwitz*, 1993; *Wise et al*., 2008). The efflorescence RH (ERH) is the point at which the particle releases the water originally taken up and the substance transforms from an aqueous liquid into a crystalline solid phase. Because efflorescence requires nucleation, there is a hysteresis effect and the ERH is often well below the DRH. For a glass, taking up and releasing water vapor occurs through a different process. Ideally, the water uptake of a glass should be the same as for a liquid; as the RH is increased the particle absorbs water until thermodynamic equilibrium is reached. However, with a glass the equilibrium time-scale is so long due to slow diffusion that the particle takes up water only on the outer monolayers. As the RH is increased, more and more layers take up water inducing a self-accelerating process and a gradual deliquescence until the particle becomes a viscous liquid. This process has been termed a humidity induced glass transition and occurs at RH_g (*Burnett et al*., 2004; *Mikhailov et al*., 2009). It has been hypothesized there would be a water gradient with different refractive indices through the glassy particle as it takes up more water until the glass transition (*Koop et al*., 2011). A recent paper modeled the hypothesis of a water uptake gradient and also a core-shell model with the water/glassy shell and a glassy core using a mixture of sucrose and NaCl particles

(*Bones et al*., 2012). The core-shell model had a better fit to the data, suggesting a water uptake model of a core-shell with different refractive indices for the two regions.

It has been shown in previous studies that glasses will likely form in the atmosphere as the temperature and RH of the atmosphere oscillates (*Zobrist et al*., 2008). An improved understanding of the hygroscopic optical growth of glassy aerosols is also needed to better understand the behavior and implications of glasses in the atmosphere. In this study, we explore the RH glass transition of mixed inorganic and glass forming organic particles at room temperature. The optical growth of the particles is measured as the RH is increased from 0-85% RH. Results show that the main impact of the glass is inhibition of AS crystallization, which in turn has a significant impact on the hygroscopic growth.

3.2 Experimental Methods

Cavity ring-down aerosol extinction spectroscopy (CRD-AES), shown in Figure 3.1, was used to determine optical growth at 532 nm. This system has been extensively detailed in previous work (*Baynard et al*., 2006; *Baynard et al*., 2007; *Beaver et al*., 2010; *Beaver et al*., 2008; *Pettersson et al*., 2004). Briefly, a pulsed Nd:YAG laser with 532 nm light, which is coupled to wet and dry cells that are each capped with highly reflective mirrors (R > 99.998%, Advanced Thin Films). The time it takes for the light entering the cells to decay was measured with no aerosol present (τ_0, sec) and with aerosol present (τ, sec). The aerosol extinction in both the dry and wet cells was calculated from

$$b_{\text{ext}}(\text{Mm}^{-1}) = \frac{R_L}{c}\left(\frac{1}{\tau} - \frac{1}{\tau_0}\right) \quad (3.1)$$

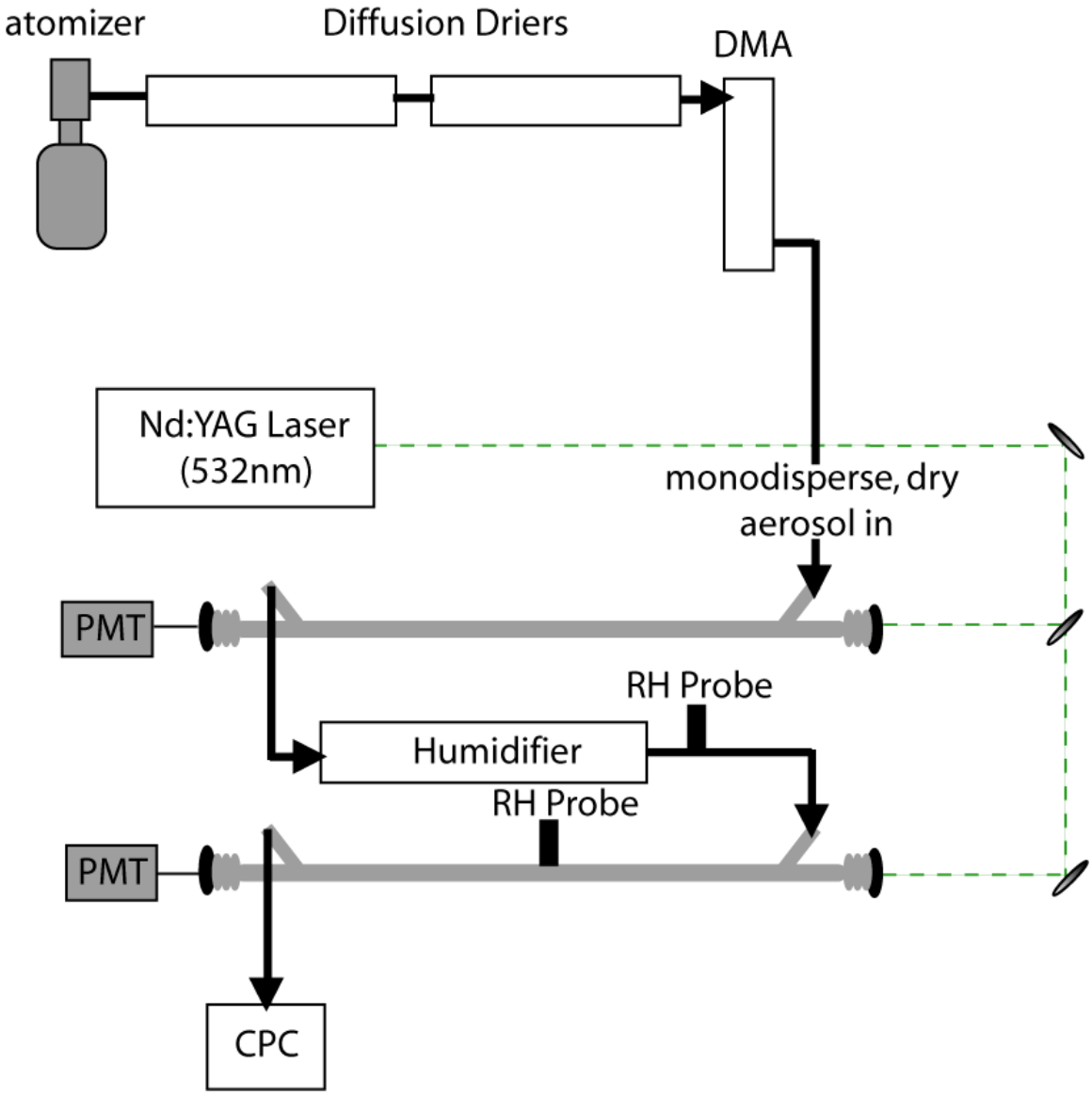

Figure 3.1 Schematic of the experimental set-up used for particle generation and to measure extinction.

where c is the speed of light (Mm/sec) and R_L is the ratio of the whole cavity length to the length that the aerosol sample occupies.

Particles are generated using an atomizer (TSI 3076) and then dried by a series of driers to an RH <10%. At room temperature, the atomization and drying process creates glassy sucrose and raffinose particles. In contrast, drying pure AS results in crystalline particles and dry pure 1,2,6-hexanetriol results in liquid particles. The dry particles are size selected using a differential mobility analyzer (DMA, TSI model 3081) to produce a monodispersed aerosol. The size-selected particles first flow into the dry cell where the ring-down time is measured. The particles then flow into a temperature-controlled humidification cell and are exposed to RH values between 5 – 85%. The RH is ramped throughout the experiment by adding small amounts of water into the heated humidification cell over a period of ~40 mins, until the RH has reached 85%. The average ramping rate is 0.76 RH%/min. The humidification cell is a stainless steel tube, containing a water vapor-permeable membrane surrounded by liquid water as the water is added to the humidifier. Following humidification, the particles flow into the wet cell where the ring-down time is again measured. The RH and temperature are monitored with Vaisala Humitter 50Y probes (±3% accuracy) immediately following the humidification cell and within the wet cell. The reading from the RH in the wet cell is used throughout the study. The two calculated extinction values are then used to calculate the $f\mathrm{RH}_{\mathrm{ext}}$ from

$$f RH_{ext}(\mathrm{RH\%, dry}) = \frac{b_{ext}(wet)}{b_{ext}(dry)} \tag{3.2}$$

to describe the optical growth of the particles. Finally, the particle concentration is measured as the particles flow into the condensation particles counter (CPC, TSI 3775).

The instrumental setup to obtain both optical images and Raman spectra of 1:1 and 2:1 AS: raffinose has been previously described in detail (*K. J. Baustian et al.*, 2010; *Schill and Tolbert*, 2012). Briefly, a Nicolet Almega XR has been equipped with a Linkham THMS600 environmental cell and Buck Research CR-1A chilled-mirror hygrometer. The spectrometer is coupled to an Olympus BX51 research grade optical microscope and is operated in reflection mode. Particles are generated by aspirating the solution of AS/raffinose with a Meinhard TR-50 glass concentric nebulizer onto a hydrophobically treated quartz disc. The nebulized droplets are allowed to coagulate on the quartz disc into supermicron droplets. The disc is then placed into the environmental cell and exposed to ~0% RH at 298 K. This evaporated the water in the droplets, resulting in AS/raffinose particles ranging in size from 2-60 μm.

Four pure compounds were used in the study: ammonium sulfate (Fisher Scientific, Certified ACS, granular), 1,2,6-hexanetriol (Sigma-Aldrich, 96%), sucrose (Mallinckrodt Chemicals, Certified ACS, crystal), and D-(+)-raffinose penta-hydrate (Sigma, ≥98.0%). All solutions were prepared using HPLC grade water and total solution concentrations were between 1.0-3.5 wt%.

3.3 Results and Discussion

Figure 3.2 shows the optical growth, $f\mathrm{RH}_{\mathrm{ext}}$, as a function of RH for pure ammonium sulfate, raffinose, sucrose, and 1,2,6-hexanetriol. Ammonium sulfate is known to have a well-

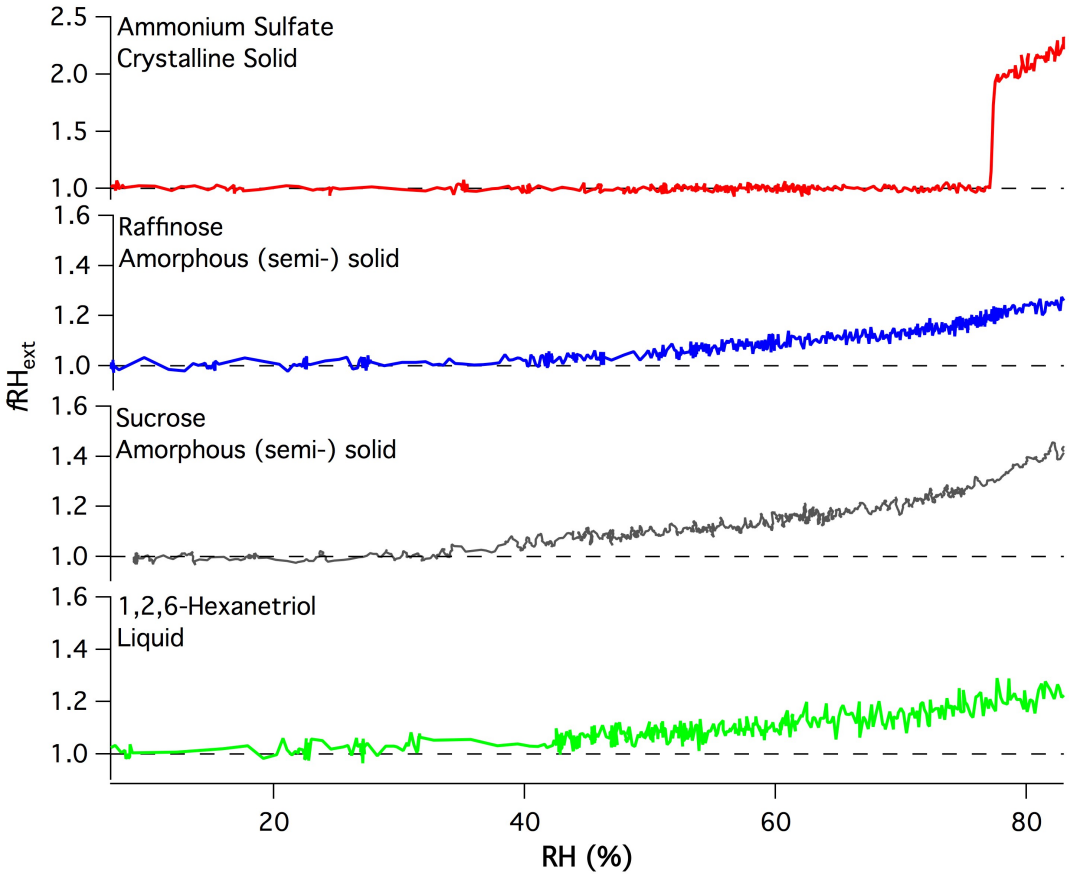

Figure 3.2 $f\mathrm{RH}_{\mathrm{ext}}$ for pure crystalline ammonium sulfate (red), amorphous (semi-) solid raffinose (blue), amorphous (semi-) solid sucrose (gray), and liquid 1,2,6-hexanetriol (green) as a function of relative humidity.

defined DRH ~ 80%.(*Martin*, 2000) In the present study, there is a prompt increase in $f\mathrm{RH}_{ext}$ at RH ~ 78%, which implies particle deliquescence and agrees with previous studies within the error (*Martin*, 2000). In contrast to the AS,1,2,6-hexanetriol has a steady increase in $f\mathrm{RH}_{ext}$ from 33.5-85% RH. 1,2,6-hexanetriol is liquid at room temperature; therefore, as soon as it is exposed to RH, there is no kinetic hindrance and it takes up water. However, the low water solubility dictates that there is not significant, measureable water uptake until an RH of 33.5%. The water uptake onset is defined as the RH_{onset} in our system. In each experiment an $f\mathrm{RH}_{ext}$ baseline signal level was determined for the initial system RH ≤ 5%. RH_{onset} is the RH at which the calculated $f\mathrm{RH}_{ext}$ data are consistently greater than the $f\mathrm{RH}_{ext}$ baseline signal plus the experimental noise. The signal/noise at the RH_{onset} is ~ 50. For both sucrose and raffinose, there is no water uptake until ~34% RH for sucrose ~40% RH for raffinose. After water uptake begins, there appears to be continuous water uptake from 34 or 40-85% RH. This is consistent with the humidity induced phase transition which occurs around 30-40% RH, followed by a self-accelerating water uptake process (*Zobrist et al*., 2011).

Figure 3.3 shows the RH_{onset} as a function of particle size for pure sucrose. The RH_{onset} at each particle size is very similar. Within the experimental error water uptake occurs at 35%±5% RH for particle diameters in the range 200-500nm. Because each particle size within our size range is yielding a similar RH_{onset}, only 300 nm particles were used for the rest of this study. The RH_{onset} range and average for all of the pure substances and mixtures are listed in Table S1. In the experimental set-up used, the RH increases rapidly up to 20%. With this fast rate of increase, accurate RH_{onset} reading could not be made below 20% RH.

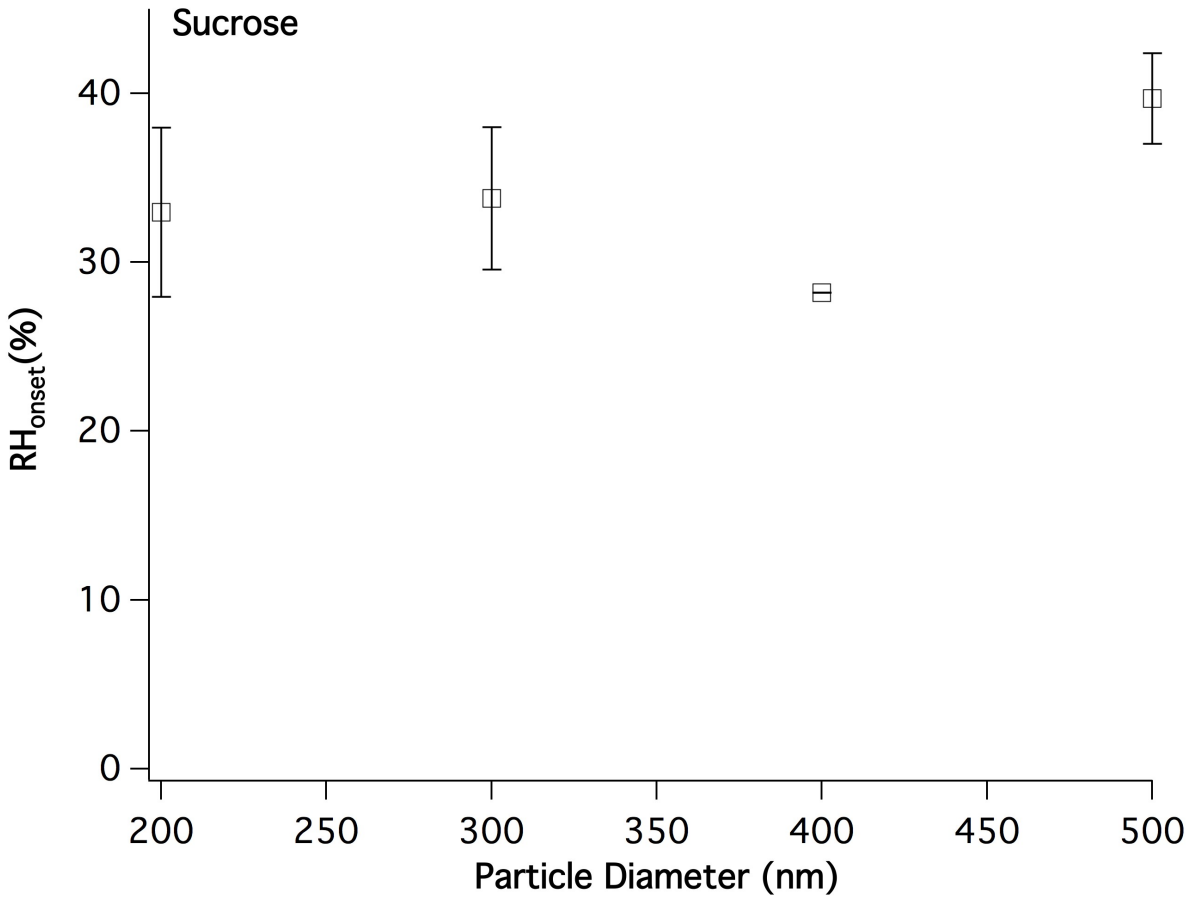

Figure 3.3 The RH_{onset} for pure sucrose particles with varying diameters. The error comes from multiple experiments ramping the relative humidity at the same particle size.

For each of the pure compounds, the hygroscopic growth factor was calculated. Hygroscopic growth factor (Gf) is defined as the wet particle diameter divided by the dry particle diameter at a specific RH, $Gf = D_{wet} / D_{dry}$. Mie theory was used to calculate Gf by calculating the extinction for particles whose diameter ranges from the dry diameter to 2.25 times the dry diameter. The water volume needed to cause this change in size was calculated and used to calculate $f\mathrm{RH}_{ext}$. The $f\mathrm{RH}_{ext}$ values were them compared to the experimental values, and the diameter with the best match was used to determine the physical growth (*Hasenkopf et al*., 2011). The calculated Gf of the pure compounds are in Table 3.1.

Figure 3.4 shows the $f\mathrm{RH}_{ext}$ for pure ammonium sulfate, pure raffinose, and three mixtures of ammonium sulfate and raffinose. As was previously shown, AS exhibits no growth until deliquescence with a DRH ~77.5%. For the 2:1 AS:raffinose mixture, there is very little water uptake before deliquescence is observed at RH ~ 75%. Previous studies have shown that mixtures including AS and an organic component with a lower RH_{onset} than AS DRH, will have a lower combined DRH (*Brooks et al*., 2003). Our value of DRH = 75% is consistent with these observations. The 1:1 and 1:2 AS:raffinose mixtures behave similarly to each other. Here, it appears there is enough raffinose in the mixtures that it is inhibiting AS crystallization. Thus water uptake by AS can occur at RH below the DRH. The $f\mathrm{RH}_{ext}$ of the 1:1 mixture is larger than the 1:2 mixture, because it contains more AS. For pure raffinose, there is steady water uptake similar to the 1:1 and 1:2 mixtures, but with less water uptake.

To test the hypothesis that water uptake can occur by AS below the DRH in the 1:1 and 1:2 AS:raffinose mixtures, Raman microscopy studies were performed to determine the particle phase of the mixtures. Figure 3.5a and 3.5b show the optical images of 1:1 and 2:1 AS:raffinose particles exposed to ~0% RH at 298K for at least 10 minutes. The 1:1 AS:raffinose particle

Substance	Relative Humidity	Refractive Index	Growth Factor	*f*RH
AS	60	1.53	1.00	1.00
	70	1.53	1.00	1.00
	80	1.53	1.35	2.09
Raffinose	60	1.676	1.05	1.11
	70	1.676	1.07	1.15
	80	1.676	1.11	1.25
Sucrose	60	1.656	1.05	1.11
	70	1.656	1.08	1.17
	80	1.656	1.10	1.24
1,2,6-Hexanetiol	60	1.478	1.02	1.05
	70	1.478	1.03	1.09
	80	1.478	1.05	1.14
2:1 AS and sucrose	60	1.56	1.03	1.01
	70	1.56	1.03	1.07
	80	1.56	1.27	1.69
1:1 AS and sucrose	60	1.59	1.13	1.28
	70	1.59	1.18	1.40
	80	1.59	1.25	1.60
1:2 AS and sucrose	60	1.61	1.10	1.23
	70	1.61	1.13	1.31
	80	1.61	1.20	1.47
2:1 AS and raffinose	60	1.59	1.00	1.00
	70	1.59	1.02	1.04
	80	1.59	1.32	1.69
1:1 AS and raffinose	60	1.6	1.14	1.29
	70	1.6	1.19	1.40
	80	1.6	1.29	1.62
1:2 AS and raffinose	60	1.63	1.10	1.18
	70	1.63	1.13	1.26
	80	1.63	1.21	1.40

Table 3.1 The refractive index, growth factor and optical growth, *f*RH, at relative humidities of 60, 70, and 80% for each substance used. The refractive indices of ammonium sulfate, 1,2,6-hexanetriol, sucrose, and raffinose are well known. The calculated volume weighted refractive index was used for each mixture.

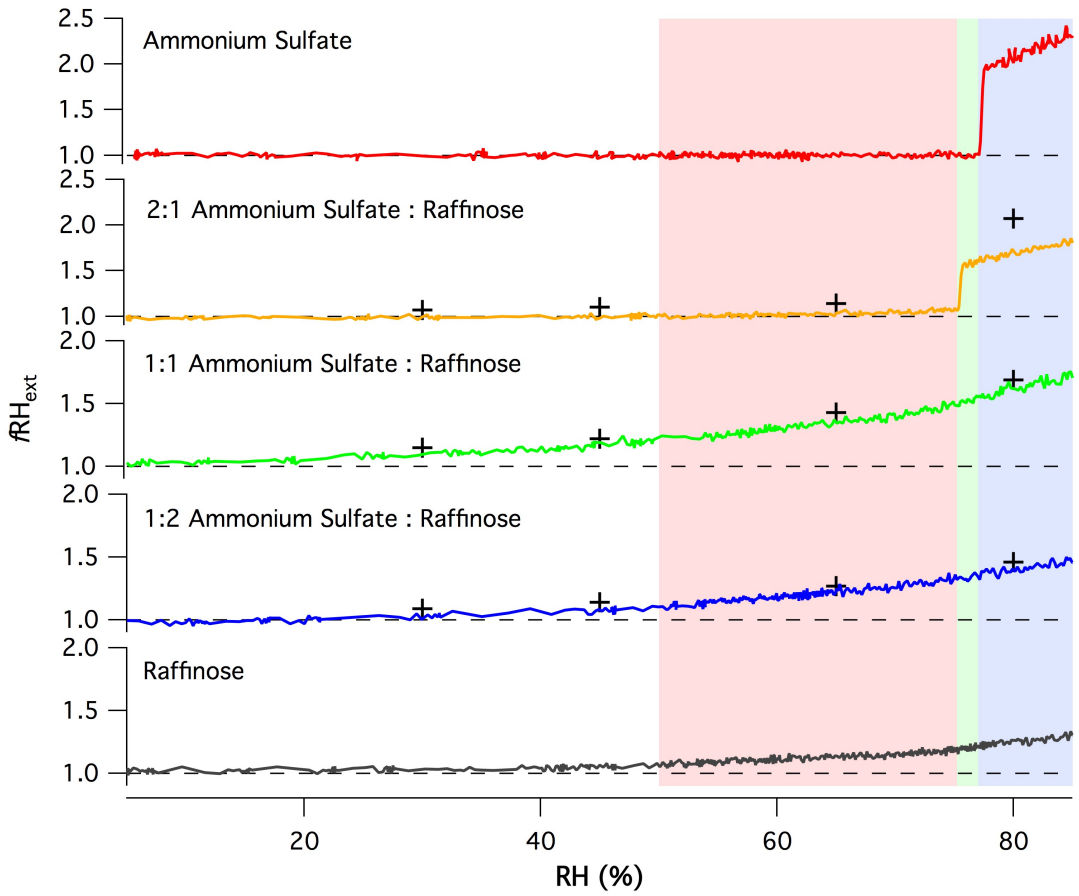

Figure 3.4 $f\mathrm{RH}_{ext}$ for pure crystalline ammonium sulfate (red), 2:1 mixture of crystalline ammonium sulfate and amorphous (semi-) solid raffinose (yellow), 1:1 mixture of amorphous (semi-) solid raffinose sulfate particles (green), 1:2 mixture of amorphous (semi-) solid raffinose sulfate particles (blue), and pure amorphous (semi-) solid raffinose (gray) as a function of relative humidity. Model data (+) calculated using volume weighted optical growth factors (Gf) of the pure ammonium sulfate and raffinose.

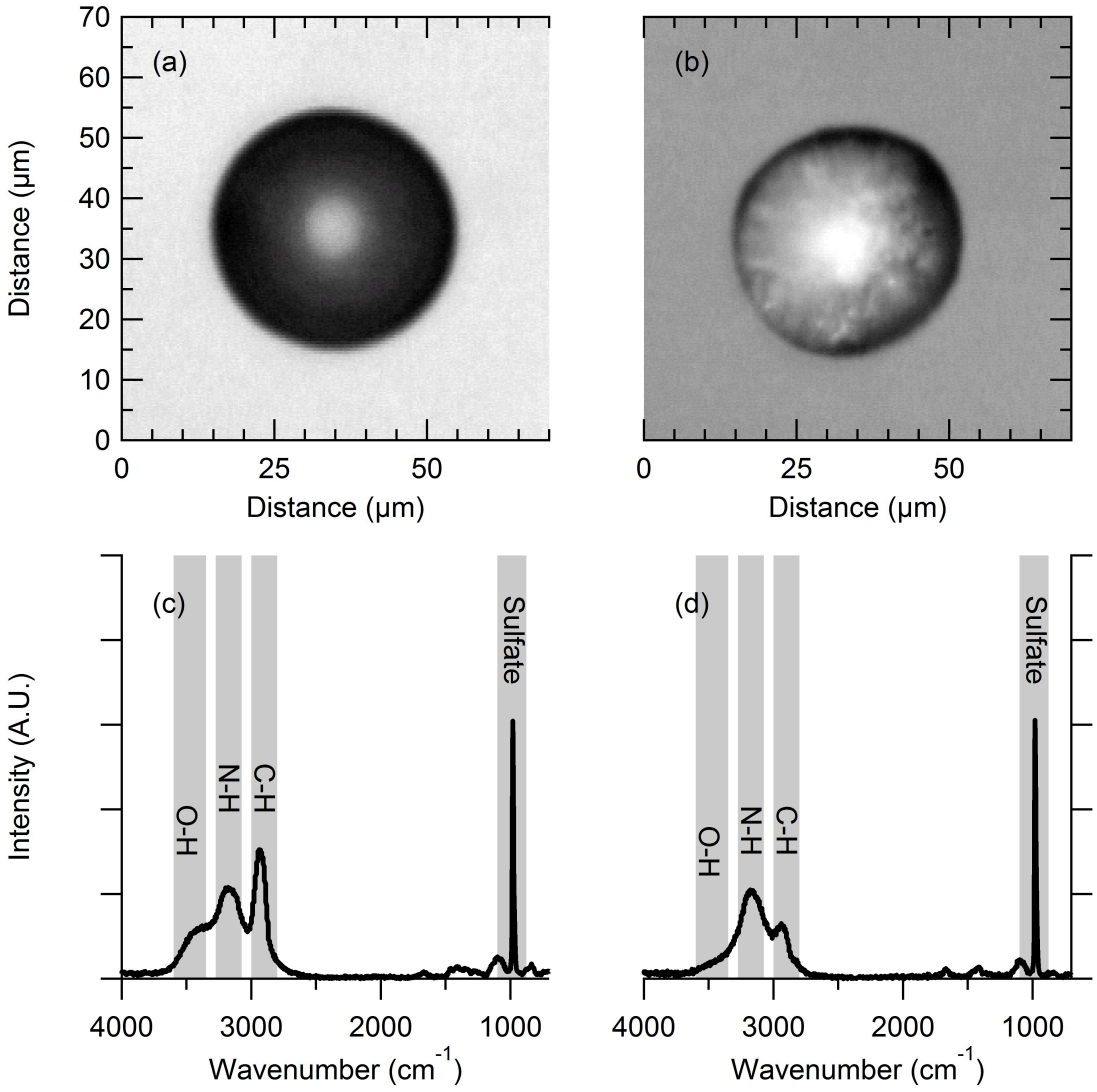

Figure 3.5 Optical images for (a) a dry mixture particle of 1:1 ammonium sulfate and raffinose and (b) a dry mixture particle of 2:1 ammonium sulfate and raffinose, both at room temperature. The Raman line maps for (c) the same dry mixture particle of 2:1 ammonium sulfate and raffinose and (d) the same dry mixture particle of 1:1 ammonium sulfate and raffinose.

exhibits a spherical morphology without any internal structure, suggesting that it is in a liquid or amorphous (semi-) state. In contrast, the 2:1 AS:raffinose particle is slightly aspherical and exhibits a high degree of internal structure, suggesting that at least part of the particle is in a crystalline state. Additionally, Raman spectra of 1:1 and 2:1 AS and raffinose particles have been taken and are shown in Figure 3.5c and 3.5d. Both spectra have been normalized to the intensity of the sulfate peak. From the broad C-H and O-H peaks, we can conclude that neither particle contains a detectable amount of crystalline raffinose, as determined using a reference spectrum for crystalline raffinose.

The + symbols in Figure 3.4, are a theoretical model for $f\mathrm{RH}_{\mathrm{ext}}$, at 30, 45, 65, and 80% RH for the mixed AS and raffinose systems. Using the $f\mathrm{RH}_{\mathrm{ext}}$ data from pure AS and pure raffinose, Gf were determined at each RH for each substance. Using the Gf of the pure AS and raffinose and volume weighted them for the different mixtures, the water volume taken up by the mixed particles was calculated. The model assumes a homogeneous mixture. The wet diameter was determined by adding up the total particle volume (including the AS, raffinose, and water fractions), assuming a spherical particle. The RI for the homogenous mixture was also needed to create the model. To determine the RI of a 300 nm particles, a volume weight RI was calculated:

$$n_{wet} = \frac{V_{AS} n_{AS} + V_{Suc} n_{Suc} + V_{H_2O} n_{H_2O}}{V_{AS} + V_{Suc} + V_{H_2O}} \tag{3.3}$$

Each compound is non-absorbing, therefore k = 0. Mie codes were used to determine the theoretical extinction for both the wet and dry homogeneously mixed particles, which were then used to calculate the $f\mathrm{RH}_{\mathrm{ext}}$. The model follows the $f\mathrm{RH}_{\mathrm{ext}}$ very well for all the mixtures at most

of the RH values. For the 2:1 AS:raffinose mixture, at 80% RH, the model is slightly off. It is unclear whether this is a real effect where the sugar is inhibiting particle growth, or if it is a systematic error.

Table 3.2 shows the fRH_{ext}, calculated Gf, and the RI used to calculate the Gf, at RH = 60, 70, and 80%. For the mixtures at relative humidities below the deliquescence of the pure AS and 2:1 mixtures, there is more growth in the particles with 50% AS or less. This is due to the suppression of AS crystallization, allowing both the AS and sugar to take up water above the RH_{onset}. Above the DRH for the mixtures, there is greater growth in the particles containing more AS, because of the greater solubility of AS.

The behavior of the AS/sucrose mixtures is almost identical to that of AS/raffinose. Figure 3.6 is similar to Figure 3.4, but for AS and sucrose. The pure sucrose, pure AS, and AS and sucrose mixtures show the same behavior as the pure raffinose, pure AS and AS and raffinose mixtures. The fRH_{ext} has the same trends for each mixture. The model also fits the data well with the same exception of one point.

Previous studies have modeled the glass transitions pure sucrose, pure raffinose, and 1:1 AS:sucrose mixture. The glass transition is the point at which the particle transitions from a glass to a liquid. The RH_{onset} in these experiments is also the point at which the particles transition from a glass to a liquid. Baustain et al. (2012) modeled sucrose and 1:1 AS/sucrose data by fitting a third order polynomial equation to their experimental data. Zobrist et al. (2008) modeled pure sucrose and sucrose data by fitting sixth order polynomial equation. The sucrose, raffinose, and 1:1 AS:sucrose mixture data from this study are the RH_{onset} averages of three different experiments with the same conditions. Figure 3.7 compares the data from this study to

Substance	RH_{onset} % Average	RH_{onset} % Range
Ammonium Sulfate	77.5	77 - 78
Sucrose	33.8	30 - 38
Raffinose	39.5	37 - 41
1,2,6-Hexanetriol	33.5	32 - 34
1:1 AS and Sucrose	< 20	11 - 17
1:2 AS and Sucrose	< 20	11 - 17
2:1 AS and Sucrose	36.5	34 - 39
1:1 AS and Raffinose	< 20	12 - 16
1:2 AS and Raffinose	< 20	16 - 17
2:1 AS and Raffinose	58.4	56 - 60

Table 3.2 The average RH_{onset} and RH_{onset} range observed for 3 separate experiments for pure ammonium sulfate, pure 1,2,6-hexanetriol, pure sucrose, pure raffinose, ammonium sulfate and sucrose mixtures, and ammonium sulfate and raffinose mixtures.

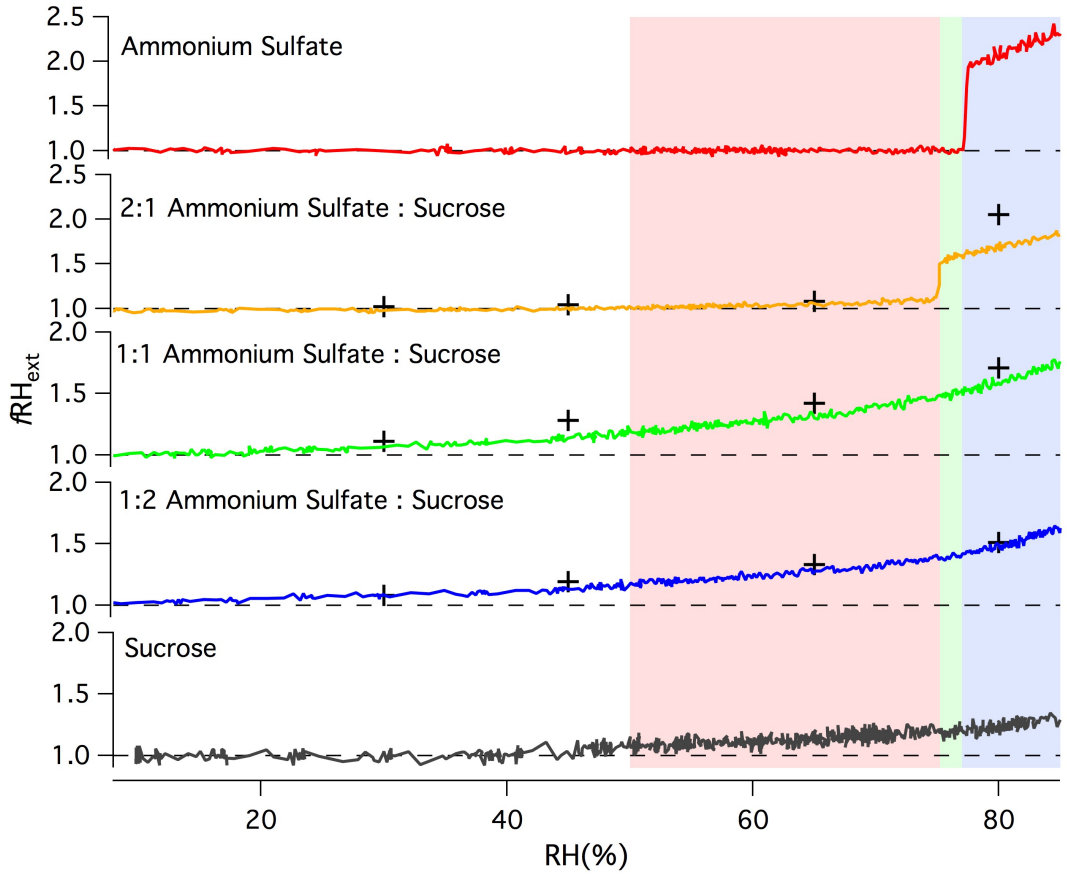

Figure 3.6 fRH_{ext} for pure crystalline ammonium sulfate (red), 2:1 mixture of crystalline ammonium sulfate and amorphous (semi-) solid sucrose (yellow), 1:1 mixture of amorphous (semi-) solid sucrose sulfate particles (green), 1:2 mixture of amorphous (semi-) solid sucrose sulfate particles (blue), and pure amorphous (semi-) solid sucrose (gray) as a function of relative humidity. Model data (+) calculated using volume weighted optical growth factors (Gf) of the pure ammonium sulfate and sucrose.

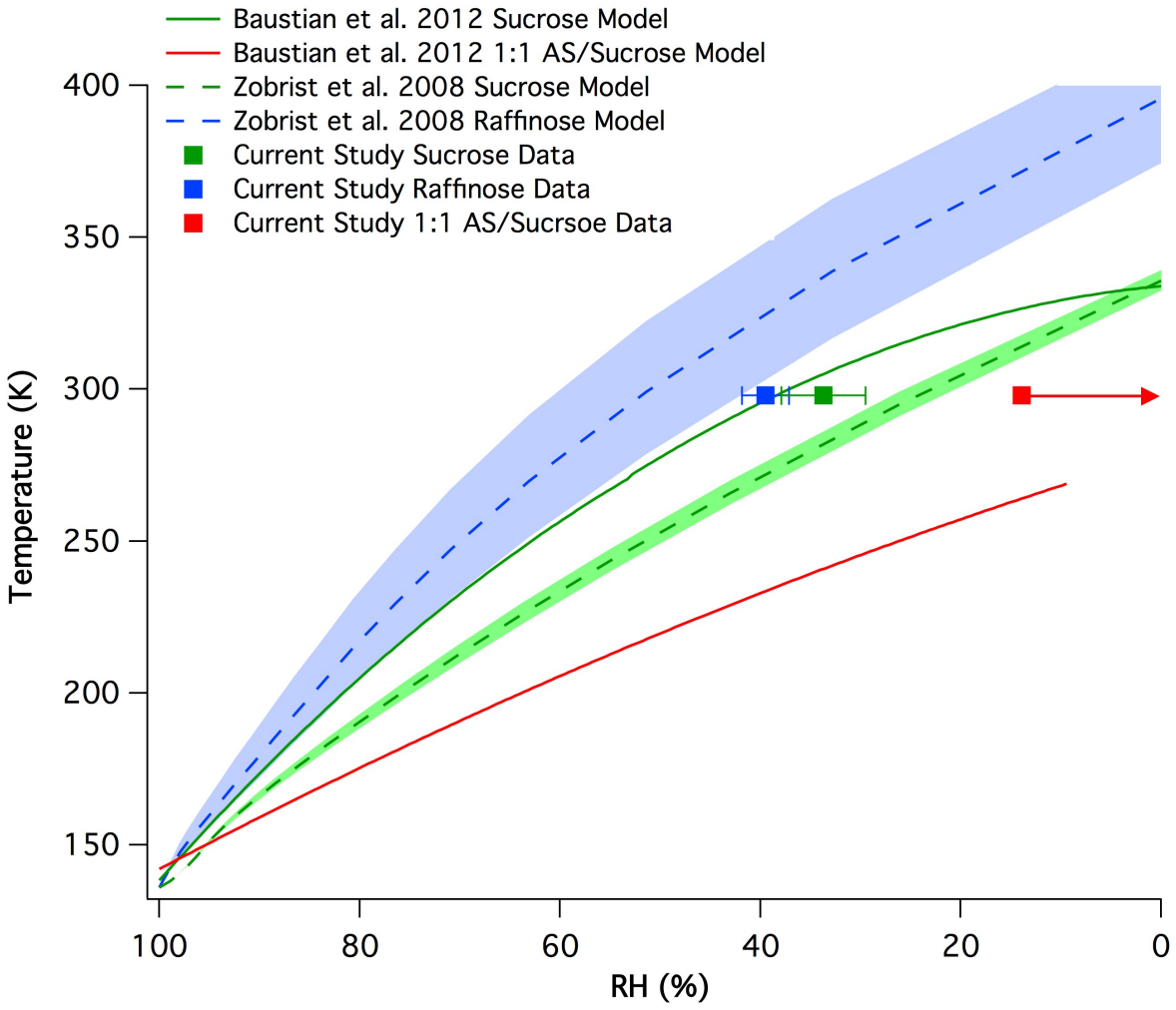

Figure 3.7 The glass transition line as temperature and relative humidity change defined by Baustain et al. 2012 for pure sucrose and 1:1 mixture of ammonium sulfate and sucrose, defined by Zobrist et al. 2008 for pure sucrose and raffinose. The RH_{onset} from the current study, at room temperature, for pure sucrose, raffinose, and the 1:1 mixture of ammonium sulfate and sucrose.

the models from the previous studies. The shaded regions around each of these glass transition curves are the associated errors calculated using the Zobrist et al. parameterizations. The pure sucrose data are closer to the Baustain et al. model line, but fall between the Baustain et al. and Zobrist et al. model. The pure raffinose data and its error overlap the Zobrist et al. model and error, suggesting that our RH_{onset} is similar to Zobrist's glass transition line at room temperature. The 1:1 mixture data from this study are quite far off from the Baustain et al. model line. The data from this study are likely an upper limit for the RH_{onset}, because in the set-up used in these experiments, the RH increases too quickly below 20% to determine an RH_{onset} below 20%.

3.4 Conclusions

In this work, the optical growth factors as a function of RH have been measured for mixtures of AS and glassy sugars. Glassy sucrose and raffinose show optical growth similar to that of a liquid, 1,2,6-hexanetriol. Although liquids immediately take up water as RH is increased, there is so little water uptake that the RH_{onset} is similar to that of glassy particles at room temperature. For the mixed particles, when the particles are completely glassy, the glassy sugars suppress AS crystallization and do not inhibit diffusion of water. This leads to more growth in these particles above their RH_{onset}, but below the DRH of the 2:1 mixture particles. At 60% RH the 1:1 mixture particles have 14% more growth than the 2:1 mixture particles. Above the DRH, at 80% RH, the 2:1 mixture has a 2% greater growth than the 1:1 mixture particles. The AS particle fraction is the most important component in understanding glassy organic sulfate particles. When particles contain more AS than organic, they act similar to a pure AS particle. In contrast, if the particle contains more organic, it acts like liquid particles. If glassy aerosol are

not taken into account in climate change models, the overall water uptake of atmospheric particle will be underestimated.

Chapter IV

Summary, Conclusions, and Future Directions

4.1 Summary and Conclusions

This thesis focused on the water uptake of mixed ammonium sulfate particles and how this uptake affected their aerosol optical properties. The data and analysis contained in this thesis should be included in climate change models to better understand climate forcing by aerosols.

In Chapter II, it was determined that to understand the water uptake of a mixed LLPS particle you need to understand the RH history of an air parcel containing those particles. The optical growth of the mixed particles is consistent with the additive mixing rules for multiple component aerosols. The water uptake of a particle as the RH is decreased, should be a function of the water uptake of its pure components. This is precisely what the data show; the mixture optical growth is between the growth of pure AS and pure 1,2,6-hexanetriol. Overall, the water uptake behavior is dictated by the phase of the AS portion of the mixed particle. For particles at room temperature, more water uptake is observed if the AS core has deliquesced allowing for the particle to liquid-liquid phase separate.

Additionally, the organic coatings are allowing water to diffuse through and not inhibiting AS crystallization. As the RH is increased for the mixed particles, there is very little water uptake, consistent with only 1,2,6-hexanetriol taking up water. If the organic coating were inhibiting crystallization, both the AS and 1,2,6-hexanetriol would take up water and there would

be a much larger optical growth than is observed in these experiments. If the coating were limiting water diffusion to the AS core, there would be limited growth at RH = 80%.

Modeling in this study showed that the expected water uptake of homogeneously mixed particles and LLPS particles is very similar. With this specific mixture, particle morphology does not change the ability of a particle to take up water. This is likely, because the RI of both the core and shell are similar to each other. For the systems where LLPS has occurred, the refractive indices for each component in the system may be similar to each other. (*Bertram et al.*, 2011) AS has a RI of 1.53, and the RI of the organic compounds used in LLPS studies range from 1.43 – 1.67. (*RSC*) The refractive index values for ammonium sulfate and 1,2,6-hexanetriol are also similar to each other. Further studies are needed to explore whether a similar core and shell refractive index are needed for LLPS to occur.

The optical growth as a function of RH was determined for pure AS, 1,2,6-hexanetriol, sucrose, raffinose, and mixtures of AS and raffinose or sucrose in Chapter III. The growth of the glassy sucrose and raffinose is similar to that of liquid 1,2,6-hexanetriol. Though liquids immediately take up water as RH is increased, there is little water uptake by the 1,2,6-hexanetriol before RH_{onset} ~ 34%. Allowing the pure glassy particles to take up water similar to a liquid would simplify the addition of glasses to climate change models.

For the mixed particles, the AS fraction of particles, is the most important component when trying to understand glassy organic sulfate atmospheric particles. When a particle contains more AS than organic, it acts similar to a pure AS particle. The AS in the mixed particle is crystalline, and the particle does not take up much water until it deliquesces. When the particle contains more organic, it acts like a liquid particle and has slow continuous water uptake. Below the DRH of the 2:1 mixtures, there is more water uptake by the glassy 1:1 and 1:2 mixtures. The

glassy sugars suppress the crystallization of AS, allowing water uptake by both the AS and 1,2,6-hexanetriol portions of the particle. Above the DRH, there is increased growth in the 2:1 mixture which is greater than the 1:1 and 1:2 mixtures. There is larger growth, because after the particles have deliquesced, as the AS portion of the particle is increased the particle has a larger hygroscopicity and take up more water.

4.2 Future Directions

Although this thesis provides a solid understanding of the optical growth for a combination of mixed aerosols, there are still many questions that remain unanswered. Further studies are needed to explore the optical growth of other mixed aerosol combinations, studies to understand the aerosol indirect effect, and studies of the wavelength-dependent growth factor.

4.2.1 Optical Properties of Other Mixed Aerosols

A previous study determined that LLPS separation occurs in multiple inorganic and organic mixtures. (*Bertram et al*., 2011) In this thesis, only one organic and inorganic combination was explored, 1,2,6-hexanetriol and ammonium sulfate. It was hypothesized that the optical growth modeled for a homogeneous mixture and a core-shell morphology were so similar, because the refractive indices of the components were very similar. More optical growth experiments for liquid-liquid phase separated mixed particles are needed to determine in this hypothesis stands for other mixed particles. Studies also need to be performed to determine if LLPS can occur in particles whose core and shell have very different refractive indices.

4.2.2 Aerosol Indirect Effect – Ice Nucleating Ability

For both the liquid-liquid phase separated and the ammonium sulfate glassy mixed particles, the direct aerosol effect was explored by determining the optical growth of these particles while varying the relative humidity. The ability to act as cloud condensation nuclei for LLPS particles is expected to be the same as pure AS. It has been previously shown that for mixed inorganic/organic particles there is not enhanced CCN activity besides that from size and solubility effects. (*Abbatt et al*., 2005) With a quick diffusion time and the LLPS particles acting like a homogeneous mixture, it is not expected for the CCN activity to be affected in LLPS particles. Although this is expected, further studies are needed to explore if the cloud condensation nuclei ability of these particles is affected by the LLPS. The experimental set-up to determine the CCN ability is already used in the Tolbert group and explained in great detail in Baustian et al. (2010). (*K. J. Baustian et al.*, 2010). Multiple studies from our group have begun exploring both the nucleation ability of glassy mixture and LLPS particles. (*K. J. Baustian et al.*, 2012; *Schill and Tolbert*, 2012) Both studies are limited in scope. Only one LLPS mixture was explored, and only 1:1 weight % glassy ammonium sulfate mixtures were explored. Further experiments exploring the CNN ability of other LLPS mixtures and other weight % would be of interest.

4.2.3 Optical Properties of Atmospheric Aerosols at λ= 405 nm

A λ = 405 nm CRD-AES has been built in addition to the CRD-AES at λ = 532 nm. The instrumentation and software for the λ= 405 nm are the same as for the λ = 532 nm. The only

differences are in the wavelength dependent CRD-AES mirrors, table optics used in the set-up, and photomultiplier tube optics.

With the current experimental set-up, only the refractive index at λ = 405 nm can be determined. With the addition of a second λ = 405 nm cell, the optical growth and growth factor could be determined. It would be ideal to conduct all of the previous experiments at both wavelengths. Determining the optical growth wavelength-dependent incoming solar radiation would add another dimension to these data. In addition, it would also be useful in climate change models to understand the wavelength dependent growth. It would also be a great system check, because the optical growth for the two wavelengths would be different, but the retrieved growth factor should be the same since it is a physical property of the particles. If the retrieved growth factors were the same, it would prove our system to be very robust.

Bibliography

Abbatt, J. P. D., K. Broekhuizen, and P. P. Kumal (2005), Cloud condensation nucleus activity of internally mixed ammonium sulfate/organic acid aerosol particles, *Atmospheric Environment*, *39*(26), 4767-4778.

Abbatt, J. P. D., S. Benz, D. J. Cziczo, Z. Kanji, U. Lohmann, and O. Mohler (2006), Solid ammonium sulfate aerosols as ice nuclei: A pathway for cirrus cloud formation, *Science*, *313*(5794), 1770-1773.

Aldrich Chemical Company, I. (1996), 1,2,6-Hexanetriol Technical Bulletin, edited.
Angell, C. A. (1995), Formation of Glasses from Liquids and Biopolymers, *Science*, *267*(5206), 1924-1935.

Baustian, K. J., M. E. Wise, and M. A. Tolbert (2010), Depositional ice nucleation on solid ammonium sulfate and glutaric acid particles, *Atmospheric Chemistry and Physics*, *10*(5), 2307-2317.

Baustian, K. J., M. E. Wise, E. J. Jensen, G. P. Schill, M. A. Freedman, and M. A. Tolbert (2012), State transformations and ice nucleationin glassy or (semi-)solid amorphous organic aerosol, *Atmospheric Chemistry and Physics Discussions*, *12*, 27333–27366.

Baynard, T., R. M. Garland, A. R. Ravishankara, M. A. Tolbert, and E. R. Lovejoy (2006), Key factors influencing the relative humidity dependence of aerosol light scattering, *Geophysical Research Letters*, *33*(6).

Baynard, T., E. R. Lovejoy, A. Pettersson, S. S. Brown, D. Lack, H. Osthoff, P. Massoli, S. Ciciora, W. P. Dube, and A. R. Ravishankara (2007), Design and application of a pulsed cavity ring-down aerosol extinction spectrometer for field measurements, *Aerosol Science and Technology*, *41*(4), 447-462.

Beaver, M. R., M. A. Freedman, C. A. Hasenkopf, and M. A. Tolbert (2010), Cooling Enhancement of Aerosol Particles Due to Surfactant Precipitation, *Journal of Physical Chemistry A*, *114*(26), 7070-7076.

Beaver, M. R., R. M. Garland, C. A. Hasenkopf, T. Baynard, A. R. Ravishankara, and M. A. Tolbert (2008), A laboratory investigation of the relative humidity dependence of light extinction by organic compounds from lignin combustion, *Environmental Research Letters*, *3*(4).

Bertram, A. K., S. T. Martin, S. J. Hanna, M. L. Smith, A. Bodsworth, Q. Chen, M. Kuwata, A. Liu, Y. You, and S. R. Zorn (2011), Predicting the relative humidities of liquid-liquid phase separation, efflorescence, and deliquescence of mixed particles of ammonium sulfate, organic material, and water using the organic-to-sulfate mass ratio of the particle and the oxygen-to-carbon elemental ratio of the organic component, *Atmospheric Chemistry and Physics*, *11*(21), 10995-11006.

Bohren, C. F., and D. R. Huffman (1983), *Absorption and Scattering of Light by Small Particles*, John Wiley & Sons, Inc.

Bones, D. L., J. P. Reid, D. M. Lienhard, and U. K. Krieger (2012), Comparing the mechanism of water condensation and evaporation in glassy aerosol, *Proceedings of the National Academy of Sciences of the United States of America*, *109*(29), 11613-11618.

Brooks, S. D., M. E. Wise, M. Cushing, and M. A. Tolbert (2002), Deliquescence behavior of organic/ammonium sulfate aerosol, *Geophysical Research Letters*, *29*(19).

Brooks, S. D., R. M. Garland, M. E. Wise, A. J. Prenni, M. Cushing, E. Hewitt, and M. A. Tolbert (2003), Phase changes in internally mixed maleic acid/ammonium sulfate aerosols, *Journal of Geophysical Research-Atmospheres*, *108*(D15).

Burnett, D. J., F. Thielmann, and J. Booth (2004), Determining the critical relative humidity for moisture-induced phase transitions, *International Journal of Pharmaceutics*, *287*(1-2), 123-133.

Chang, E. I., and J. F. Pankow (2006), Prediction of activity coefficients in liquid aerosol particles containing organic compounds, dissolved inorganic salts, and water - Part 2: Consideration of phase separation effects by an X-UNIFAC model, *Atmospheric Environment*, *40*(33), 6422-6436.

Ciobanu, V. G., C. Marcolli, U. K. Krieger, U. Weers, and T. Peter (2009), Liquid-Liquid Phase Separation in Mixed Organic/Inorganic Aerosol Particles, *Journal of Physical Chemistry A*, *113*(41), 10966-10978.

Clegg, S. L., K. S. Pitzer, and P. Brimblecombe (1992), Thermodynamics of Multicomponent, Miscible, Ionic-Solutions. 2. Mixtures Including Unsymetrical Electrolytes

, *Journal of Physical Chemistry*, *96*(23), 9470-9479.

Clegg, S. L., P. Brimblecombe, and A. S. Wexler (1998), Thermodynamic model of the system H+-NH4+-SO42--NO3--H2O at tropospheric temperatures, *Journal of Physical Chemistry A*, *102*(12), 2137-2154.

Clegg, S. L., J. H. Seinfeld, and P. Brimblecombe (2001), Thermodynamic modelling of aqueous aerosols containing electrolytes and dissolved organic compounds, *Journal of Aerosol Science*, *32*(6), 713-738.

Cziczo, D. J., J. B. Nowak, J. H. Hu, and J. P. D. Abbatt (1997), Infrared spectroscopy of model tropospheric aerosols as a function of relative humidity: Observation of deliquescence and crystallization, *Journal of Geophysical Research-Atmospheres*, *102*(D15), 18843-18850.

Dai, Q., J. Hu, and M. Salmeron (1997), Adsorption of water on NaCl (100) surfaces: Role of atomic steps, *Journal of Physical Chemistry B*, *101*(11), 1994-1998.

Debenedetti, P. G., and F. H. Stillinger (2001), Supercooled liquids and the glass transition, *Nature*, *410*(6825), 259-267.

Dennis-Smither, B. J., K. L. Hanford, N.-O. A. Kwamena, R. E. H. Miles, and J. P. Reid (2012), Phase, Morphology, and Hygroscopicity of Mixed Oleic Acid/Sodium Chloride/Water Aerosol Particles before and after Ozonolysis, *Journal of Physical Chemistry A*, *116*(24), 6159-6168.

Erdakos, G. B., and J. F. Pankow (2004), Gas/particle partitioning of neutral and ionizing compounds to single- and multi-phase aerosol particles. 2. Phase separation in liquid particulate matter containing both polar and low-polarity organic compounds, *Atmospheric Environment*, *38*(7), 1005-1013.

Erdakos, G. B., E. I. Chang, J. F. Pankow, and J. H. Seinfeld (2006), Prediction of activity coefficients in liquid aerosol particles containing organic compounds, dissolved inorganic salts, and water - Part 3: Organic compounds, water, and ionic constituents by consideration of short-, mid-, and long-range effects using X-UNIFAC.3, *Atmospheric Environment*, *40*(33), 6437-6452.
Finlayson-Pitts, B. J., Pitts, J.N. (2000), *Chemistry in the Upper and Lower Atmosphere: Theory, Experiments and Applications*, Academic, San Diego, London.

Forster, P., Ramaswamy, V., Artaxo, P., Berntsen, T., Betts R., et al. (2007), Climate Change 2007: The Physical Scientific Basis, in *Fourth Assessment Report of the Intergovernmental Panel on Climate Change*, edited, Cambridge University Press, Cambridge, United Kingdom and New York, NY, USA.

Freedman, M. A., C. A. Hasenkopf, M. R. Beaver, and M. A. Tolbert (2009), Optical Properties of Internally Mixed Aerosol Particles Composed of Dicarboxylic Acids and Ammonium Sulfate, *Journal of Physical Chemistry A*, *113*(48), 13584-13592.

Garland, R. M., A. R. Ravishankara, E. R. Lovejoy, M. A. Tolbert, and T. Baynard (2007), Parameterization for the relative humidity dependence of light extinction: Organic-ammonium sulfate aerosol, *Journal of Geophysical Research-Atmospheres*, *112*(D19).

Hasenkopf, C. A., M. A. Freedman, M. R. Beaver, O. B. Toon, and M. A. Tolbert (2011), Potential Climatic Impact of Organic Haze on Early Earth, *Astrobiology*, *11*(2), 135-149.

Hasenkopf, C. A., M. R. Beaver, M. G. Trainer, H. L. Dewitt, M. A. Freedman, O. B. Toon, C. P. McKay, and M. A. Tolbert (2010), Optical properties of Titan and early Earth haze laboratory analogs in the mid-visible, *Icarus*, *207*(2), 903-913.

Jimenez, J. L., et al. (2009), Evolution of Organic Aerosols in the Atmosphere, *Science*, *326*(5959), 1525-1529.

Koop, T., J. Bookhold, M. Shiraiwa, and U. Poschl (2011), Glass transition and phase state of organic compounds: dependency on molecular properties and implications for secondary organic aerosols in the atmosphere, *Physical Chemistry Chemical Physics*, *13*(43), 19238-19255.

Krieger, U. K., C. Marcolli, and J. P. Reid (2012), Exploring the complexity of aerosol particle properties and processes using single particle techniques, *Chemical Society Reviews*, *41*(19), 6631-6662.

Marcolli, C., and U. K. Krieger (2006), Phase changes during hygroscopic cycles of mixed organic/inorganic model systems of tropospheric aerosols, *Journal of Physical Chemistry A*, *110*(5), 1881-1893.

Martin, S. T. (2000), Phase transitions of aqueous atmospheric particles, *Chemical Reviews*, *100*(9), 3403-3453.

Mikhailov, E., S. Vlasenko, S. T. Martin, T. Koop, and U. Poschl (2009), Amorphous and crystalline aerosol particles interacting with water vapor: conceptual framework and experimental evidence for restructuring, phase transitions and kinetic limitations, *Atmospheric Chemistry and Physics*, *9*(24), 9491-9522.

Murphy, D. M., D. J. Cziczo, K. D. Froyd, P. K. Hudson, B. M. Matthew, A. M. Middlebrook, R. E. Peltier, A. Sullivan, D. S. Thomson, and R. J. Weber (2006), Single-particle mass spectrometry of tropospheric aerosol particles, *Journal of Geophysical Research-Atmospheres*, *111*(D23).

Pankow, J. F. (2003), Gas/particle partitioning of neutral and ionizing compounds to single- and multi-phase aerosol particles. 1. Unified modeling framework (vol 37, pg 3323, 2003), *Atmospheric Environment*, *37*(35), 4993-4993.

Parsons, M. T., D. A. Knopf, and A. K. Bertram (2004), Deliquescence and crystallization of ammonium sulfate particles internally mixed with water-soluble organic compounds, *Journal of Physical Chemistry A*, *108*(52), 11600-11608.

Pettersson, A., E. R. Lovejoy, C. A. Brock, S. S. Brown, and A. R. Ravishankara (2004), Measurement of aerosol optical extinction at 532nm with pulsed cavity ring down spectroscopy, *Journal of Aerosol Science*, *35*(8), 995-1011.

Pratt, K. A., and K. A. Prather (2010), Aircraft measurements of vertical profiles of aerosol mixing states, *Journal of Geophysical Research-Atmospheres*, *115*.

Reid, J. P., B. J. Dennis-Smither, N. O. A. Kwamena, R. E. H. Miles, K. L. Hanford, and C. J. Homer (2011), The morphology of aerosol particles consisting of hydrophobic and hydrophilic phases: hydrocarbons, alcohols and fatty acids as the hydrophobic component, *Physical Chemistry Chemical Physics*, *13*(34), 15559-15572.

Royal Society of Chemistry (January 2013), The Free Chemical Database, http://www.chemspider.com/

Schill, G. P., and M. A. Tolbert (2012), Heterogeneous ice nucleation on phase-separated organic-sulfate particles: effect of liquid vs. glassy coatings, *Atmospheric Chemistry and Physics Discussion*, *12*(12), 30951-30988.

Seinfeld, J. H., Pandis S.N. (2006), *Atmospheric Chemistry and Physics*, Wiley Interscience, Hoboken, NJ.

Shindo, H., M. Ohashi, O. Tateishi, and A. Seo (1997), Atomic force microscopic observation of step movements on NaCl(001) and NaF(001) with the help of adsorbed water, *Journal of the Chemical Society-Faraday Transactions*, *93*(6), 1169-1174.

Smith, M. L., M. Kuwata, and S. T. Martin (2011), Secondary Organic Material Produced by the Dark Ozonolysis of alpha-Pinene Minimally Affects the Deliquescence and Efflorescence of Ammonium Sulfate, *Aerosol Science and Technology*, *45*(2), 244-261.

Song, M., C. Marcolli, U. K. Krieger, A. Zuend, and T. Peter (2012), Liquid-liquid phase separation and morphology of internally mixed dicarboxylic acids/ammonium sulfate/water particles, *Atmospheric Chemistry and Physics*, *12*(5), 2691-2712.

Stokes, R. H., and R. A. Robinson (1966), Interactions in Aqueous Nonelectrolyte Solutions. I. Solute-Solvent Equilibria, *Journal of Physical Chemistry*, *70*(7), 2126-&.

Tang, I. N., and H. R. Munkelwitz (1993), Composition and Temperature-Dependence of the Deliquescence Properties of Hygroscopic Aerosols *Atmospheric Environment Part a-General Topics*, *27*(4), 467-473.

Wexler, A. S., and S. L. Clegg (2002), Atmospheric aerosol models for systems including the ions H+, NH4+, Na+, SO42-, NO3-,Cl-, Br-, and H2O, *Journal of Geophysical Research-Atmospheres*, *107*(D14).

Wise, M. E., S. T. Martin, L. M. Russell, and P. R. Buseck (2008), Water uptake by NaCl particles prior to deliquescence and the phase rule, *Aerosol Science and Technology*, *42*(4), 281-294.

You, Y., et al. (2012), Images reveal that atmospheric particles can undergo liquid-liquid phase separations, *Proceedings of the National Academy of Sciences of the United States of America*, *109*(33), 13188-13193.

Zarzana, K. J., D. O. De Haan, M. A. Freedman, C. A. Hasenkopf, and M. A. Tolbert (2012), Optical Properties of the Products of alpha-Dicarbonyl and Amine Reactions in Simulated Cloud Droplets, *Environmental Science & Technology*, *46*(9), 4845-4851.

Zhang, Q., et al. (2007), Ubiquity and dominance of oxygenated species in organic aerosols in anthropogenically-influenced Northern Hemisphere midlatitudes, *Geophysical Research Letters*, *34*(13).

Zobrist, B., C. Marcolli, D. A. Pedernera, and T. Koop (2008), Do atmospheric aerosols form glasses?, *Atmospheric Chemistry and Physics*, *8*(17), 5221-5244.

Zobrist, B., V. Soonsin, B. P. Luo, U. K. Krieger, C. Marcolli, T. Peter, and T. Koop (2011), Ultra-slow water diffusion in aqueous sucrose glasses, *Physical Chemistry Chemical Physics*, *13*(8), 3514-3526.

Zuend, A., C. Marcolli, T. Peter, and J. H. Seinfeld (2010), Computation of liquid-liquid equilibria and phase stabilities: implications for RH-dependent gas/particle partitioning of organic-inorganic aerosols, *Atmospheric Chemistry and Physics*, *10*(16), 7795-7820.